

THE LUMINESCENCE RESPONSE OF PHOSPHORS
TO POSITIVE ION BOMBARDMENT

AN EXPERIMENTAL STUDY
OF THE
LUMINESCENCE RESPONSE OF PHOSPHORS
TO
POSITIVE ION BOMBARDMENT

By
CLIFFORD FREDERICK EVE, B.Sc.

A Thesis
Submitted to the Faculty of Arts and Science
in Partial Fulfilment of the Requirements
for the Degree
Doctor of Philosophy

McMaster University

October 1957

DOCTOR OF PHILOSOPHY (1957)
(Physics)

McMASTER UNIVERSITY
Hamilton, Ontario.

TITLE: An Experimental Study of the Luminescence Response
of Phosphors to Positive Ion Bombardment

AUTHOR: Clifford Frederick Eve, B.Sc. (University of London)

SUPERVISOR: Professor H.E. Duckworth

NUMBER OF PAGES: v, 60

NUMBER OF FIGURES: 27

SCOPE AND CONTENTS:

This thesis describes experiments in which the luminescence response of two phosphors, ZnS:Ag and $\text{Zn}_2\text{SiO}_4:\text{Mn}$, to positive ion bombardment was studied. In the first chapter an account of the apparatus and general experimental procedure is given. The second chapter is devoted to a consideration of the effect of the thickness of the phosphor sample. Chapters III and IV deal with the effect of the energy and nature of the bombarding ions. A theoretical interpretation of the experimental results is presented.

Acknowledgements

I am greatly indebted to my supervisor, Professor H.E. Duckworth, for his interest and advice throughout the course of this work. It is also a pleasure to acknowledge the encouragement and guidance given by the members of my supervisory committee, Dr. H.E. Petch and Dr. A.T. Hutcheon. Dr. R.H. Tomlinson, who was a frequent guest at the meetings of this committee, was to a large extent responsible for the original suggestion of the subject of this work. My thanks are also due to Dr. P.R. Zilsel for helpful discussion in connection with the theoretical aspect of the work. Valuable assistance was given by Arie van Wijngaarden in the preparation of the phosphor samples and also during some of the experiments. I am very grateful to Gertrude Isenor for her assistance in the drawing of the diagrams for this thesis.

This work was supported by the Ontario Research Foundation, the U.S. Air Force through the Air Force Office of Scientific Research and Development Command, and the National Research Council of Canada.

I am indebted to the Ontario Research Foundation and to the Shell Oil Company of Canada for the award of post-graduate scholarships during the course of this work.

Contents

	Page
Introduction	1
Chapter I - Apparatus and Experimental Procedure	8
1. Brief Description	8
2. Ion Source	9
3. Acceleration and Collimation of the Ion Beam	14
4. Analysis of the Beam	15
5. Measurement of Ion Current	17
6. Phosphor Samples	17
7. Detection of Luminescence	19
8. Vacuum System	21
Chapter II - The Effect of Sample Thickness	22
1. Experiment	22
2. Results	22
3. Theory	22
4. Comparison of Experiment with Theory ...	27
Chapter III - The Effect of Ion Energy and Type of Ion	31
1. The Form of the Energy Dependence	31
2. Variation with the Nature of the Bombarding Ions	34
3. The Effect of Deterioration	39
4. Deterioration with Very Low Energy Ions..	42
Chapter IV - Discussion of the Results of Chapter III	45
1. Efficiency	45
2. Interpretation of E_0	47
3. Theory	49
4. Comparison of Theory with Experiment ...	54
Summary	58
References	60

List of Figures

		following page
Figs. 1 - 3	Figures for Chapter I	21
Fig. 4	Figure for Chapter II	30
Figs. 5 - 25	Figures for Chapter III	44
Figs. 26 - 27	Figures for Chapter IV	57

Introduction

When a substance is excited by the absorption of energy, this energy must be dissipated if the substance is to revert to its original state. If this dissipation involves the emission of light not forming a component of thermal radiation, the process is known as luminescence. Solid luminescent materials are referred to as phosphors.

Luminescence can be excited by the absorption of energy in many different forms, e.g. ultra violet radiation, X-radiation, cathode rays and positive rays. Most of the fundamental experiments that have led to elucidation of the mechanism of luminescence emission have been performed with U.V. excitation. This is because such excitation produces a minimum of additional effects in the phosphor which might mask or complicate the luminescence. Also, by suitable choice of wavelength, it is possible to confine the excitation to selected electronic transitions. This gives to the experiments a measure of control that is not afforded by other means of excitation.

Phosphors may be classified into three groups according to the mechanism of their luminescence. The first group consists of materials which are luminescent in the pure state. In these materials electronic transitions are induced in the lattice by the exciting radiation, and the

reverse transitions give rise to the luminescence emission. For a given transition the absorption wavelength is generally less than the emission wavelength (Stokes' law), so that in many cases the luminescence quanta can escape from the phosphor without strong absorption. Among the best known materials of this group are the tungstate phosphors.

The phosphors of the first group include only a small fraction of the commonly known crystals. It is therefore concluded that in most crystals non-radiative de-excitation usually follows electronic excitation, the excitation energy being dissipated in the form of thermal vibrations of the lattice. A model for such a process has been suggested by Seitz (1939). However, many substances that are non-luminescent in the pure state can be endowed with luminescence properties by the addition of small quantities of impurities. The role of the activating impurity atoms is to provide centres in which the electron energy is sufficiently decoupled from that of the lattice vibrations to allow radiative de-excitation to compete with the non-radiative process. The impurity activated phosphors form the second and third groups of the present classification.

The second group comprises those phosphors that, under U.V. excitation, give rise to luminescence through direct absorption and re-emission by electronic transitions in the luminescence centres formed by the activating

impurity. In the phosphors of this group the excitation and emission spectra are both dependent on the nature of the activator. Examples of phosphors of this group are the thallium activated alkali halides and also manganese activated zinc orthosilicate, one of the phosphors used in the experiments described in this thesis.

The third group, which includes the sulphide phosphors, consists of impurity activated phosphors in which, under U.V. excitation, energy is absorbed in the lattice of the host crystal and transported to the luminescence centres which become ionized. The luminescence centres give rise to localized electron energy levels situated in the normally forbidden energy region between the valence and conduction bands of the crystal. The absorption of energy in the lattice produces free electrons in the conduction band and free holes in the valence band. The existence of these free charge carriers during excitation of the phosphor is confirmed by the appearance of photoconductivity which always accompanies luminescence in these phosphors. A hole migrating through the crystal can be captured into a luminescence centre which consequently becomes ionized. The ionized centre can then capture an electron from the conduction band and so return to its original un-ionized condition. There is not general agreement as to which stage of the above process produces the luminescence quantum.

According to the model used by Klasens (1946) for the sulphide phosphors, the activator gives rise to localized electron levels situated just above the top of the valence band. When one of these levels is ionized by the capture of a hole from the valence band an infra-red quantum is supposed to be emitted. The luminescence quantum is attributed to the subsequent capture of an electron from the conduction band by the ionized centre. An alternative model has been proposed by Lambe and Klick (1955) who assume that the impurity level is situated just below the bottom of the conduction band and that the luminescence quantum is the result of the capture of the hole by the centre, so that emission coincides with ionization of the centre. The ionized centre then captures a conduction electron to return to its original state. Lambe and Klick (1955) and Lambe (1955) offer a considerable weight of experimental evidence in favour of their model.

When a phosphor is excited by bombardment with corpuscular rays most of the incident energy is absorbed in the first instance by the host lattice, for the absorption is non-resonant and is divided between the host crystal and the activator according to their respective molecular concentrations. Hence, if appreciable luminescence is excited by this means, a mechanism of energy transport between the host lattice and the luminescence centres such

as that described above must be operative. Under corpuscular bombardment, however, electronic excitation is not the only mechanism by which the incident energy can be absorbed in the crystal. A competing process is provided by the possibility of elastic collisions whereby some of the incident energy is imparted to the lattice atoms in the form of vibrational energy. If sufficient energy is transferred in a single collision, an atom may be permanently displaced from its normal site in the lattice. Such displacements are thought to produce centres at which the non-radiative recombination of free electrons and holes can occur (see, for example, Martin 1957). It is probable that these centres trap electrons (or holes) for a sufficient period of time to allow the probability of eventual non-radiative recombination to become large. In the meantime the capture of the trapped electrons (or holes) by the luminescence centres is prevented. The luminescence efficiency of a phosphor consequently declines under prolonged ion bombardment due to the formation of lattice defects. In the range of ion energies used in the experiments described in this thesis, elastic collisions constitute the dominant mechanism of energy loss (see Seitz 1949). Thus the bombardment results in only a small amount of luminescence but can, if suitably prolonged, give rise to considerable deterioration of the phosphor. For this

reason, most of the previous work concerning the bombardment of phosphors with low energy ions has been devoted to a study of the modifications of the luminescence properties of the phosphor produced by the bombardment rather than to the luminescence response itself. Smith and Turkevich (1954) give a comprehensive list of references to work concerning the effect of α particle bombardment on the luminescence properties of ZnS phosphors. Smith and Turkevich themselves investigated the modifications produced in ZnS:Cu by neutron bombardment. In addition to this work the deterioration of luminescence efficiency of phosphors under low energy ion bombardment has been studied by Hanle and Rau (1952), Berthold (1955) and Young (1955). Martin (1957) has made a detailed study of the effect of prolonged H_2^+ ion bombardment on many of the properties of phosphors.

The only previous work known to the writer in which the luminescence response of phosphors to low energy ion bombardment has been studied as a function of the ion energy is that of Hanle and Rau (1952). These authors found that under H_2^+ ion bombardment the luminescence response of ZnS:Ag was approximately proportional to the ion energy for energies between 15 and 35 KeV. Broser and Warminsky (1951) investigated the luminescence response of a CdS phosphor to α particles from polonium and reported that the luminescence was proportional to the incident energy. In their experi-

ment, however, it was the total incident energy that was varied while the energy per α particle remained constant. Richards and Hays (1950) introduced a scintillation detector in their time of flight mass spectrometer, and some general observations were made concerning the light output as a function of ion energy for K^+ and Rb^+ ions with energies up to 30 KeV. However, in subsequent work with this instrument the scintillation detector was replaced by an electron multiplier.

The work described in this thesis was initiated with a view to the possible development of a scintillation detector of 50 - 100 KeV positive ions in a high resolution mass spectrometer constructed by Prof. H.E. Duckworth and his group in this laboratory. As the work proceeded, however, this application was lost sight of, partly because, as in the work of Richards and Hays, an electron multiplier was found to be a very satisfactory detector in the mass spectrometer and partly because the writer's interest in the more fundamental aspects of the project was stimulated in the early stages of the work. The project was therefore continued as a fundamental investigation of the luminescence response of phosphors to positive ion bombardment.

Chapter I

Apparatus and Experimental Procedure

At the beginning of this chapter a brief overall description of the apparatus will be given. Various features of the apparatus and experimental procedure will then be described in more detail section by section.

1. Brief Description

The general principle of operation of the apparatus is illustrated diagrammatically in fig. 1, which shows the apparatus in its original form. Various details of the apparatus were found to require modification. Fig. 2 shows the upper portion of the apparatus in its final form.

The ion source, shown at A in fig. 1, is located at the lower extremity of the apparatus. The ions produced by this source are accelerated upwards by an electrostatic field applied between the electrodes D and E. The ions are then collimated into a narrow beam by the slits S_1 and S_2 . The direction of the ion beam can be controlled by adjusting the screw rods C which control the curvature of the bellows B_1 . The ion beam can be collected in a small Faraday cup F. The ion current to the cup is measured by means of a vibrating reed electrometer. By extending

the bellows B_2 , the Faraday cup can be retracted from the beam to permit the ions to pass on to the phosphor samples. These consist of thin layers of powdered phosphor deposited on microscope cover glasses. These glasses are mounted, phosphor side down, in holes in the horizontal brass disc G. The holes are arranged around the disc close to its periphery. By rotation of the dial H, the sample disc may be rotated so as to bring any desired phosphor sample into the path of the ion beam. Light emitted from the phosphor, after transmission through the glass backing, passes through a lucite window J which is sealed into the lid of the sample turret K. This light is then detected by a photomultiplier. The apparatus is evacuated by pumps connected via the side tube shown.

2. Ion Source

The ion source was built into the inner member of a 55/50 standard taper ground glass joint shown at L in fig. 1. By separation of the joint the source could be removed as a single unit from the remainder of the apparatus. The use of a standard taper joint permitted the direct substitution of alternative sources. The absence of any metal flange associated with this joint facilitated the insulation of the source against external breakdown of the accelerating voltage applied to it.

For the experiments with ions of the alkali metals a thermal ion source was used. The principle of operation of this source is illustrated by the inset at the right hand side of fig. 2. The filament M consisted of a strip of metallic ribbon 0.040" wide, 0.001" thick, and about 1" in length. This strip was bent into the form of an almost complete circle in a horizontal plane. The inner surface of the filament was coated with a thin layer of a salt of the alkali metal of which ions were to be produced. To obtain lithium ions, a coating of spodumene, a naturally occurring alumino-silicate of lithium, was used. To obtain Na^+ , K^+ or Rb^+ ions a coating of the sulphate of the appropriate metal was used. The filament was heated by passing a current through it. Positive ions emitted from the coated surface were impelled towards the central axis of the source by a positive potential applied to the cylinder S surrounding the filament, and drawn upwards by a negative potential applied to the electrode D. Those ions escaping through the central aperture in D passed into the accelerating field. A constant potential difference of 90 volts was maintained between S and D by the battery shown in fig. 2. The potential of the filament could be adjusted over a range intermediate between the potentials of S and D by means of the helipot P. Adjustment of this helipot provided a convenient means of controlling the ion

current delivered by the source. With the filament at a potential of a few volts below that of S, a maximum ion current was obtained. When the potential of the filament was lowered to some 35 volts below that of S the ion emission was suppressed altogether. With the filament potential intermediate between the optimum and cut-off values, the resistor R provided a measure of negative feedback which helped to stabilize the emission current from the filament. Any increase in the emission current caused a corresponding increase in the potential drop across R, thus lowering the potential of the filament relative to S, and so impeding the increase in ion current. The value of R which was found experimentally to give the best stabilization was about 1 megohm.

In the original arrangement used, the heating current for the filament was supplied from a Sola constant voltage transformer via the high voltage isolating transformer T. Because of the critical dependence of the ion current on filament temperature in this type of source, however, it was found that this arrangement did not give a sufficiently steady ion current. A considerable improvement in the stability of the ion current was obtained by replacing the Sola and isolating transformers with a high capacity 2 volt storage battery. This latter arrangement was used in most of the experiments reported in this thesis.

A rheostat having a maximum resistance of 1 ohm was inserted in series with the storage battery and the filament to provide a coarse control of the ion current. Fine control was achieved by adjustment of the helipot P as explained above.

The filament material used in the initial stages of this work was a commercial grade of tungsten. It was found, however, that this material contained potassium as an impurity, and that the ion current consisted predominantly of potassium ions regardless of the identity of the material coated on the surface of the filament. Thus when the filament was coated with spodumene to obtain Li^+ ions, the intensity of K^+ ions in the beam was almost three orders of magnitude greater than that of Li^+ ions. Even when the majority of the K^+ ions was rejected from the Li^+ beam by magnetic analysis, the K^+ background was sufficient to invalidate the results of the experiment. For this reason a platinum filament was used when Li^+ , Na^+ or Rb^+ ions were required.

The geometry of the source was such as to minimize the intensity of light, produced by the heated filament, that escaped from the source to reach the photomultiplier. The circular form of the filament ensured that direct transmission of light from any portion of the filament through the collimating slits did not occur. The shield

S surrounding the filament greatly reduced the diffuse escape of light from the source. This was still further reduced by making the electrode D in the form of a cylinder closed at its upper end. This cylindrical cup fitted over the cylinder S leaving only the lower end of the source open. With this arrangement the response of the photomultiplier to the light from the source was less than the dark current.

For the experiments with H_2^+ and A^+ ions an electron bombardment source of conventional design¹ was used. This source had been used previously in other work in this laboratory. The writer acquired it in almost complete form and built it into the inner member of a ground glass joint for insertion into this apparatus. It was found that in order to obtain a sufficient intensity of the bombarding electron current in this source, the filament temperature had to be raised to a point at which the light from the source that reached the photomultiplier was comparable with the light produced by the phosphor samples, despite the insertion of baffles between the source and the phosphors. The procedure adopted to overcome this difficulty was to measure the total photomultiplier response as a function of ion current at a given ion energy, the ion current being varied by varying

¹See for example Dewdney (1955).

the repeller voltage in the source while the filament current remained constant. The photomultiplier response was plotted graphically as a function of ion current and a straight line was obtained. The intercept of this line at zero ion current was interpreted as the response of the multiplier to the light from the ion source, while the light output from the bombarded phosphor was obtained from the gradient of the line.

3. Acceleration and Collimation of the Ion Beam

On emerging from the source through the central aperture in electrode D (figs. 1 & 2), the ions entered the accelerating field. This field was established between electrode D of the source and the grounded electrode E (fig. 1) by applying to D a potential of several kilovolts (relative to ground) from an external high voltage supply. For most of the experiments the high voltage supply used was one constructed in this laboratory. This unit was capable of supplying a maximum voltage of about 30 KV. A commercially built high voltage supply employed in another project was occasionally available. This supply was used for a few experiments with K^+ ions to give ion energies up to about 40 KeV.

In the early stages of the work, breakdown of the accelerating voltage across the gap between electrodes D and E was encountered. The electrode separation was about

$3/8$ " and the residual pressure in the apparatus was about 10^{-5} mm Hg. The breakdown voltage was found to be approximately independent of both the electrode separation and the pressure. It was found, however, to be sensitive to the material used for the construction of the electrodes. Breakdown was finally eliminated by making the electrodes of KR monel.

The ions were collimated into a narrow beam by the slits S_1 and S_2 (fig. 1). These slits were about 0.005 " and 0.010 " wide respectively. The length of each slit was $1/8$ ". The distance between S_1 and S_2 was $3 1/8$ ".

4. Analysis of the Beam

Magnetic analysis was used to separate the various ion masses present in the beam. The analysing magnet consisted of a permanent magnetron-magnet located immediately above the flange U. The pole gap of the magnet was just sufficient to accommodate the main vertical tube of the apparatus. Adjustment of the bellows B_1 (fig. 1) by means of the screw rods C, caused the ion gun assembly (i.e., the source and collimating slits S_1 and S_2) to move in almost pure rotation about an axis in the plane of the flange U and intersecting the vertical axis of the tube. The deflection of the ion beam by the magnetic field could thus be conveniently accommodated by adjustment of the bellows. At a given ion energy the mass spectrum

could be scanned either by adjusting the bellows or by moving the magnet horizontally so as to vary the intensity of the magnetic field at the axis of the tube. In practice the latter method was found to be more convenient.

The ion peaks were identified by determining the mass ratio of adjacent peaks. This was done by measuring the accelerating voltages required to bring the two peaks successively onto the collector slit at constant deflection and constant magnetic field. The mass ratio of the two ions was then given by the inverse ratio of the two voltages. With spodumene on the filament in the ion source, the two isotopes of lithium were separated and identified in this way. In addition, the relative abundance observed for the two isotopes was close to the accepted value for lithium. Ions of the other alkali metals, i.e., Na, K, Rb and Cs, were also present in trace amounts due to impurities in the spodumene. The relative masses of these ions, determined as explained above, agreed with those of the alkali metals to within 2%.

The identification of the ion peaks corresponding to the alkali metals permitted the calibration of a scale relating lateral displacement of the magnet with ion mass at a given deflection and ion energy. This greatly facilitated the identification of ions used in subsequent experiments. The identification of A^+ and H_2^+ ions by

this method was confirmed by the observation that the corresponding ion peaks disappeared when the supply of gas to the electron bombardment source was interrupted.

5. Measurement of Ion Current

In the final form of the apparatus the Faraday cup F, which was used in the determination of the ion current, was located between the sample disc and a collector slit S_3 , as shown in fig. 2. The collector slit was 0.020" wide and $5/16$ " in length, and was located $10\frac{1}{2}$ " above the collimating slit S_2 . The Faraday cup was connected through a resistor of 10^{11} ohms to ground. To determine the ion current collected by the cup, the potential developed across the resistor was measured with a vibrating reed electrometer. A potential of -45 volts was applied to S_3 to suppress the emission of secondary electrons from the cup and to prevent secondary electrons liberated by ion bombardment of the tube between S_2 and S_3 from reaching the cup. The cup could be retracted by means of bellows to permit the ions to pass on to the phosphor samples.

6. Phosphor Samples

The phosphors used were ZnS:Ag (Sylvania Phosphor CR-20) and $Zn_2SiO_4:Mn$ (Sylvania Phosphor #161). These phosphors were supplied in the form of micro-crystalline powder. The samples were prepared by deposition of the

powder from suspension in ether onto microscope cover glasses 18 mm in diameter and about 0.1 mm thick. The heavier phosphor particles were rejected by allowing them to settle out before the introduction of a cover glass into the suspension. After deposition of a sample, the ether was removed by means of a drain cock in the bottom of the vessel. Ether was used for the suspending medium because of its low surface tension. When other liquids, e.g., distilled water or ethyl alcohol, were used, the surface tension caused the particles deposited on the glass to coagulate as the liquid surface came into contact with the sample during removal of the liquid. This difficulty was not encountered when ether was used. The phosphor particles were found to adhere satisfactorily to the cover glasses without the use of any binder, provided that reasonable care was taken in handling the samples.

In order to stabilize the potential of the samples during the ion bombardment, the microscope cover glasses were first coated with a transparent conducting layer of cadmium oxide. This coating was prepared by sputtering onto the glass a layer of metallic cadmium which was then oxidized by heating in air. During this heating process the colour of the coating changed from an opaque black to a pale transparent straw colour, and at the same time the

electrical conductivity of the coating increased by two or three orders of magnitude. The optical transmission spectrum of a glass coated in this way is shown in fig. 3 together with the transmission spectrum of an uncoated glass. These spectra were determined with a Beckman D.U. Spectrophotometer.

The samples were mounted, phosphor side down, in holes in the horizontal brass disc G (fig. 2). The holes were located around the disc close to its periphery. The disc was mounted on a vertical shaft which passed through a rotary vacuum seal in the bottom of the sample turret K. By rotation of the calibrated dial H, the sample disc could be rotated so as to bring any desired phosphor sample into the path of the ion beam.

7. Detection of Luminescence

Light emitted from the bombarded phosphor, after transmission through the phosphor layer and the glass backing, was focused onto the photocathode of a 1P21 photomultiplier by the lucite lens window J (fig. 2). The d-c. output of the photomultiplier was displayed on the chart of a Brown Elektronik Recorder.

In order to minimize the deterioration of the phosphor samples by the ion bombardment during the course of the experiments, the samples were kept in motion throughout the period of bombardment. The sample disc

was first adjusted so that no sample was in the path of the ion beam. After the ion current was determined, the Faraday cup was retracted and a phosphor sample then passed across the path of the ion beam by manual rotation of the sample disc. The Faraday cup was then re-inserted into the beam and a second determination of the ion current made. As the phosphor sample passed across the path of the ion beam, the photomultiplier produced a peak on the recorder chart, the peak height being proportional to the light output from the sample. The mean time taken to pass a sample across the path of the ion beam was about 5 sec . The direction of motion of the sample was perpendicular to the lengths of the slits, so that the irradiation was effectively distributed over a large area of the sample. In Chapter III evidence is presented to show that this technique of continuous scanning of the samples did indeed restrict the deterioration of the phosphor to negligible proportions.

In one experiment¹ with K^+ ions, measurements were made of the light output emitted from the same side of the phosphor samples as that bombarded by the ions. For this experiment the collimating slits S_1 and S_2 were replaced by circular apertures 0.014" and 0.031" in diameter respectively. The Faraday cup shown in fig. 2

¹See Chapter III, p. 32.

was removed, and the collector slit S_3 replaced by a plane mirror of metallic silver. This mirror was inclined at an angle of 45° to the axis of the tube so that light emitted from the underside of the phosphor sample was reflected out of the side-tube V. The photomultiplier was located at the end of this side-tube. A circular aperture $1/16''$ in diameter in the centre of the mirror formed the final defining aperture for the ion beam. The ion current was determined by locating a Faraday cup above the sample disc and leaving alternate holes in the disc vacant. When one of these vacant holes was aligned with the ion beam, the ions were collected in the Faraday cup.

8. Vacuum System

The vacuum system was constructed principally of metal. The ion gun was housed in glass tubing, however, to provide good electrical insulation between the source and ground. The only other non-metallic sections of the system were a glass cold trap and an R.C.A. 1949 ionization vacuum gauge, both located in the pumping line. The glass sections of the system were covered with black Electrical Scotch Tape to prevent light from entering the system.

The apparatus was evacuated with an Edwards R203 oil diffusion pump and a Welch 1400 Duo-Seal backing pump. The residual pressure in the apparatus was about 10^{-5} mm Hg.

Fig. 1

Initial form of the apparatus. For key to labelling
see text.

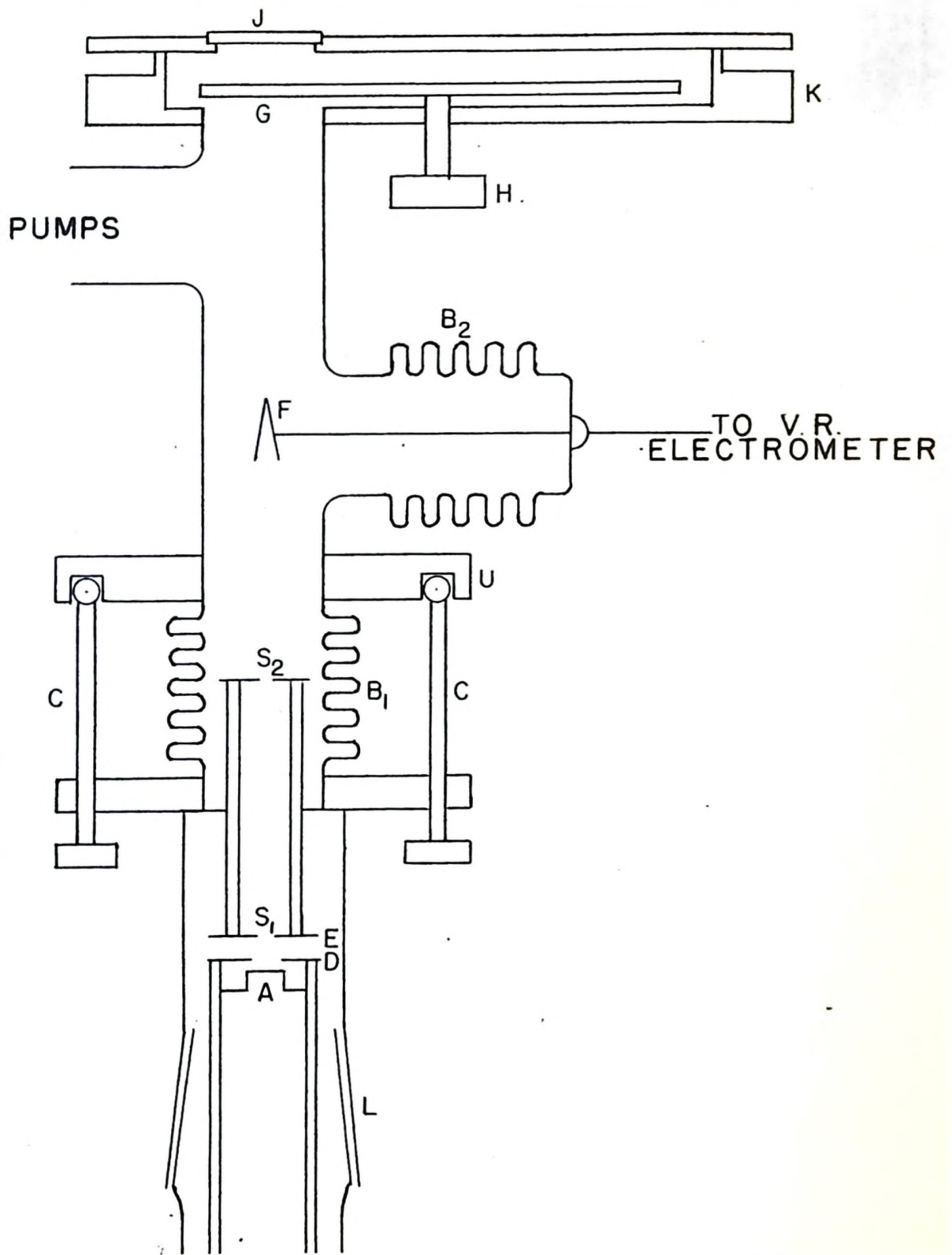
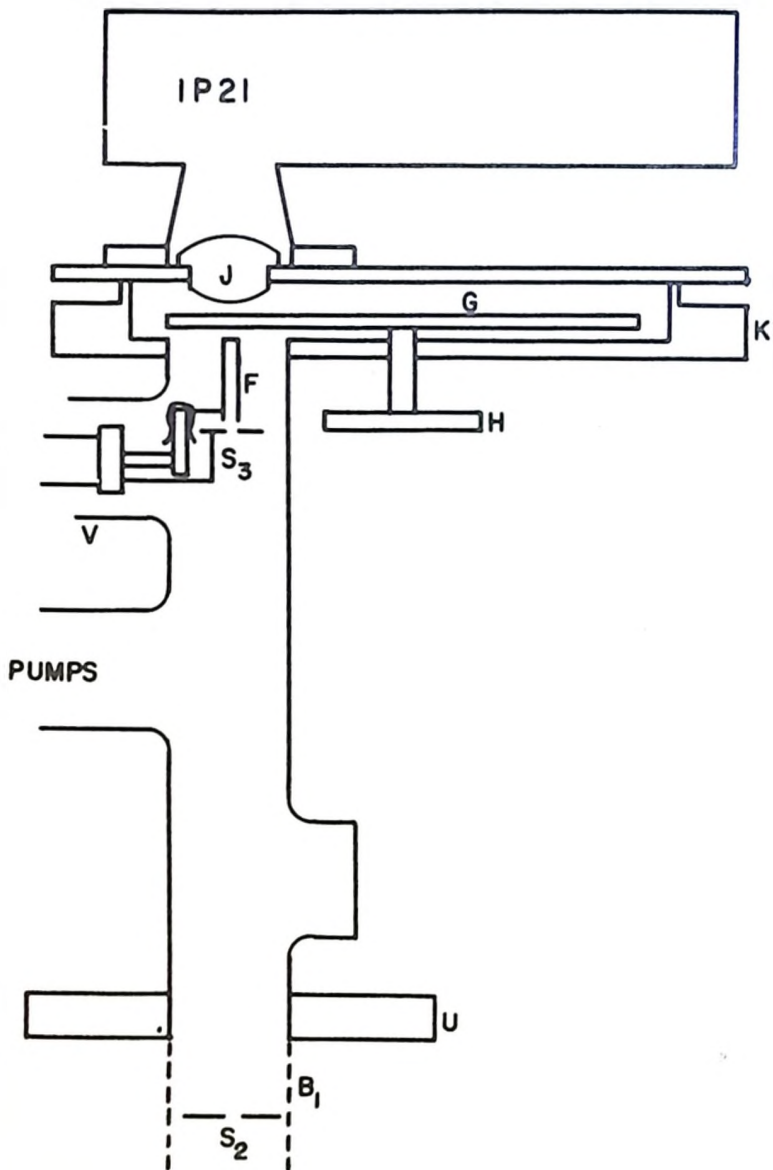


Fig. 2

Final form of the upper portion of the apparatus. The inset at the right hand side illustrates the principle of operation of the thermal ion source. Parts which are common to both figs. 1 and 2 are similarly labelled. For key to labelling see text.



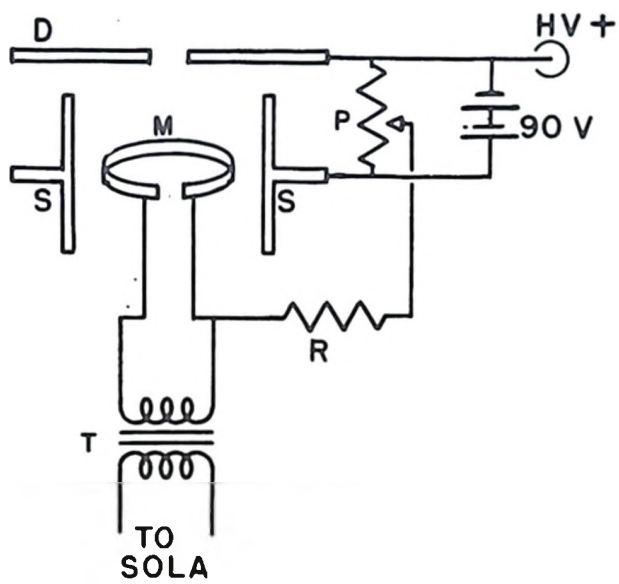
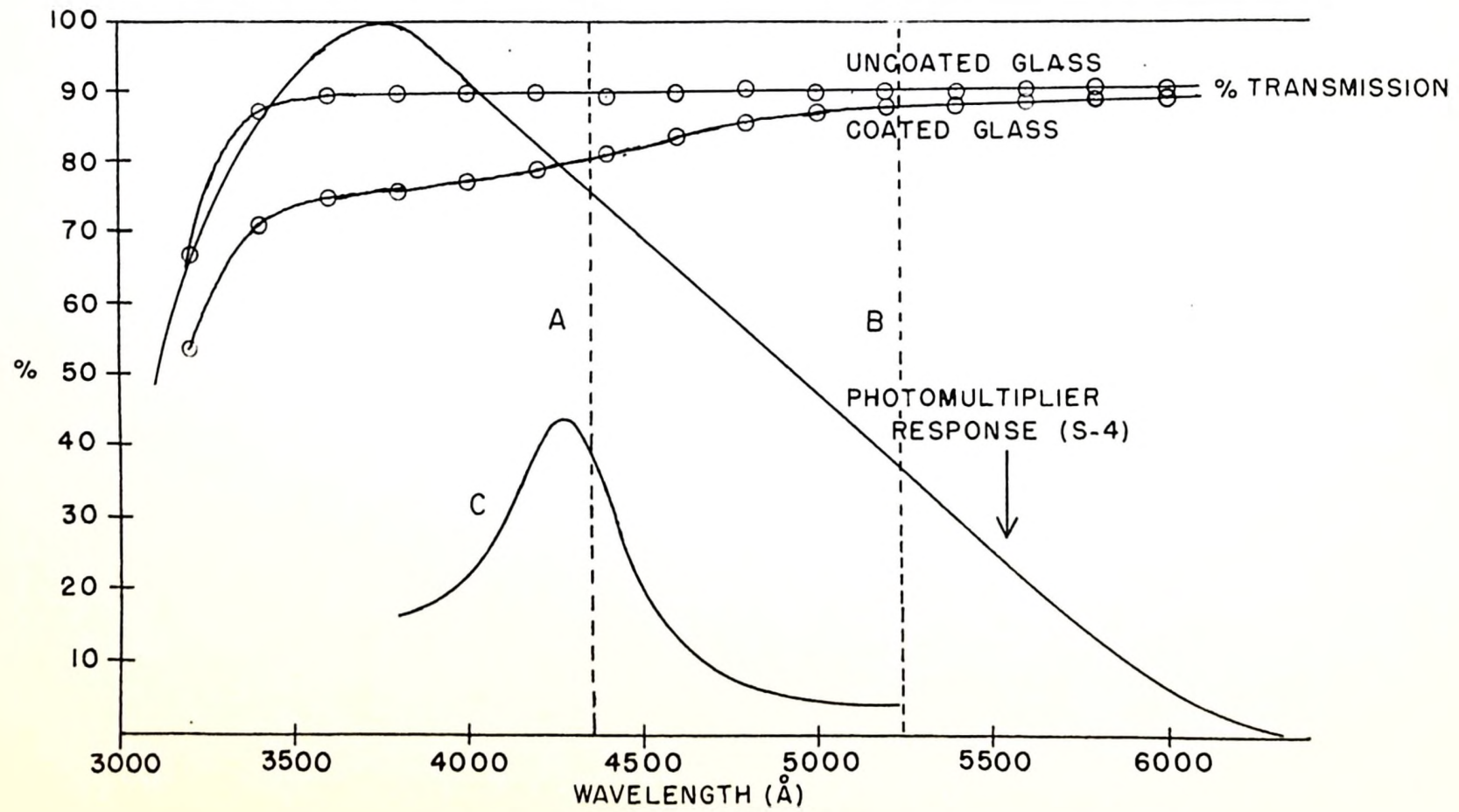


Fig. 3

The two curves for which experimental points are shown represent the effective optical transmission spectra of a coated and an uncoated microscope cover glass. The broken lines A and B represent respectively the peak emission wavelengths of ZnS:Ag (Sylvania Phosphor #CR-20) and $Zn_2SiO_4:Mn$ (Sylvania Phosphor #161) as given in the Sylvania catalogue. The S-4 response curve for the 1P21 photomultiplier is copied from the R.C.A. Tube Manual. The curve C represents the optical transmission spectrum of the filter used in the experiment with Li^{7+} ions described in Chapter III.



Chapter II

The Effect of Sample Thickness

1. Experiment

An experiment was performed in which the light emitted from samples of ZnS:Ag, under bombardment with K^+ ions, was studied as a function of sample thickness. The thickness of the samples was determined by weighing the cover glasses before and after deposition of the phosphor. Relative values of the light output, emitted from the side of the samples remote from that bombarded by the ions, were determined.

2. Results

The results of this experiment are represented by the points shown in fig. 4. There is an optimum sample thickness at which a maximum light output is obtained for a given ion energy. The value of this optimum thickness remains constant at about 2.3 mg/cm^2 for all ion energies in the range 10 - 26 KeV.

3. Theory

As the mass per unit area, or thickness, of a phosphor sample is increased from zero by progressive deposition of phosphor particles onto an initially

uncovered microscope cover glass, the light output obtainable from the sample at first increases from zero as the area of the glass covered with phosphor increases. A stage is reached, however, at which most of the area of the glass is covered, and the addition of further particles then serves principally to increase the optical absorption of the phosphor layer through which the luminescent light must pass before escaping from the remote side of the sample. It is therefore to be expected that, with increasing sample thickness, the light output will rise to a maximum and then decrease.

These considerations explain in a qualitative manner the experimental results shown in fig. 4. To obtain a more quantitative explanation of these results it is necessary to calculate the distribution of phosphor particles layer by layer as a sample is formed. With the aid of a few simplifying assumptions, such a calculation is attempted below.

Suppose that, at any stage of the deposition of a sample, the number of particles in the r th layer is n_r and the total number of particles deposited is N . Of the next dN particles to descend on the sample, a fraction dn_r/dN goes into the r th layer. This fraction is equal to the ratio of the vacant area in the r th layer to the total sample area A . The vacant area in the r th layer is

proportional to the number of particles in the $(r-1)$ th layer that are not covered by particles in the r th layer, i.e., to $(n_{r-1} - n_r)$. Hence

$$\frac{dn_r}{dN} = \frac{B(n_{r-1} - n_r)}{A}, \quad (1)$$

where B is the mean area of glass that a single particle covers.

For $r = 1$, the numerator of the right hand side of equation (1) should represent the vacant area in the first layer, which is $A - Bn_1$, i.e.,

$$\begin{aligned} B(n_0 - n_1) &= A - Bn_1, \\ \text{i.e., } n_0 &= A/B. \end{aligned} \quad (2)$$

Hence equation (1) is valid for all positive integral values of r , including $r = 1$, if n_0 is defined by equation (2). According to this definition, n_0 is the maximum number of particles that can be accommodated in a single layer.

Equation (1) can be integrated to give

$$n_r e^{BN/A} = (A/B) \int e^{BN/A} n_{r-1} dN. \quad (3)$$

Equation (3) is a reduction formula giving n_r as a function of n_{r-1} . For the case $r = 1$, the integral on the right hand side of equation (3) can be evaluated as a function

of N , with the help of equation (2). Thus n_1 can be found as a function of N . By substitution of n_1 into equation (3) with $r = 2$, n_2 can be found. Successive substitutions give n_3 , n_4 , etc. The general solution of equation (3) can then be shown by mathematical induction to be

$$n_r = (A/B) \left\{ 1 - e^{-BN/A} \sum_{m=0}^{r-1} \frac{B^m N^m}{m! A^m} \right\}. \quad (4)$$

Equation (4) satisfies the necessary condition

$$\sum_{r=1}^{\infty} n_r = N.$$

If M is the mass of phosphor per unit sample area, i.e., the sample thickness, then

$$BN/A = KM, \quad (5)$$

where K is a constant. Hence equation (4) can be written

$$n_r = (A/B) \left\{ 1 - e^{-KM} \sum_{m=0}^{r-1} (K^m M^m / m!) \right\}. \quad (6)$$

In order to calculate the light output from a sample of thickness M , it is convenient to define a quantity x_r as the area of the sample glass that is covered by r particle layers. Then

$$x_r = B(n_r - n_{r+1}). \quad (7)$$

By substitution from equation (6) for n_r and n_{r+1} , equation (7) can be written

$$x_r = \Lambda e^{-K\alpha K^r M^r / r!}. \quad (8)$$

Equation (8) satisfies the necessary condition

$$\sum_{r=0}^{\infty} x_r = \Lambda.$$

x_0 is to be interpreted as the uncovered area of the glass. It can be shown that, with this interpretation, both equations (7) and (8) are valid for $r = 0$.

Let the light intensity produced per unit covered area of the sample be I_0 . Then the light intensity emitted per unit area of the sample is given by

$$I = (1/A) \sum_{r=1}^{\infty} I_0 \alpha^r x_r, \quad (9)$$

where α is the effective optical transmission fraction of a close-packed layer. It is here assumed that the depth of penetration of the bombarding ions into the phosphor is negligible compared with the dimensions of a phosphor particle, so that all the luminescence originates in the front surface of the sample. The validity of this assumption is supported by a comparison of the measurements of Young (1955) of the ranges of various ions in ZnS:Ag, with the determination of particle size described below.

With the help of equation (8), equation (9) can be written

$$I = I_0 e^{-KM} (e^{\alpha KM} - 1). \quad (10)$$

By differentiation of equation (10), it can be shown that I has a maximum value when M has the value M_{\max} given by

$$KM_{\max} = (1/\alpha) \log_e 1/(1-\alpha). \quad (11)$$

The maximum value of I is given by

$$I_{\max} = I_0 \alpha (1-\alpha)^{(1-\alpha)/\alpha}. \quad (12)$$

4. Comparison of Experiment with Theory

The experimental points in fig. 4 were examined in order to determine M_{\max} . The value obtained was 2.28 mg/cm². The value of I_{\max} for each ion energy was determined in a similar way. A value of α was selected at random and the corresponding values of K and the I_0 's calculated from equations (11) and (12) respectively. Curves representing equation (10) for the various values of I_0 were then plotted and compared with the experimental points. This procedure was followed for several different values of α , and the value of α which led to the best fit of the theoretical curves to the experimental points was found to be 0.7. The curves shown in fig. 4 correspond to this value of α . From fig. 4 it is seen that reasonably good

agreement between theory and experiment was obtained except in the region of small sample thickness, where the experimental points corresponding to $M = 1.43 \text{ mg/cm}^2$ fall below the theoretical curves.

This discrepancy may be due to the fact that in the foregoing theory the detailed mechanism, by which the light passes through the phosphor sample and escapes from the remote side, is not considered. In practice this process will be complicated by multiple reflections at the crystal surfaces. It is not clear that the assumption, made in equation (9), of a constant transmission fraction for each close-packed particle layer is justified. Of the light which approaches the interface between two particle layers, some will pass through to the next layer, and some will be reflected back. Of this latter portion, a fraction will return to the interface after multiple reflections. This fraction will depend on the number of reflecting surfaces, and hence on the number of layers, located in front of the interface considered. These considerations suggest that, for a given layer, the effective value of α would increase with the number of layers covering the given layer. Thus for thin samples the mean value of α would be smaller than for thicker samples, and hence the relative light output for thin samples would be over-estimated by equation (10).

A further check on the validity of the theory is provided by a determination of the mean particle size. One of the phosphor samples was examined under a microscope fitted with a calibrated eye-piece scale, and the mean particle size was estimated to be approximately 4 microns.

From equation (5),

$$B = KMA/N. \quad (13)$$

If the mean mass of a particle is m , then

$$M = mn/A.$$

Hence equation (13) may be written

$$B = Km. \quad (14)$$

B is the mean geometrical area of a particle (see equation 1). Hence the mass m will be given approximately by $\rho B^{3/2}$, where ρ is the density of ZnS:Ag. In this approximation, equation (14) becomes

$$\begin{aligned} B &= K\rho B^{3/2} \\ \text{i.e., } B^{1/2} &= 1/(K\rho) \end{aligned} \quad (15)$$

With $\alpha = 0.7$ and $M_{\max} = 2.28 \text{ mg/cm}^2$, equation (11) gives $K = 0.75 \text{ cm}^2/\text{mg}$. Substituting this value of K into equation (15) and using $\rho = 4.1 \times 10^3 \text{ mg/cm}^3$, one obtains for the

approximate particle size

$$B^{1/2} = 3.3 \text{ microns.}$$

This is in good agreement with the experimentally determined value.

It is interesting to note that, according to equation (8), the uncovered area of a sample of optimum thickness is given by

$$x_0 = Ae^{-KM_{\max}} = 0.18A.$$

Hence nearly 20% of the glass must be uncovered in a sample of optimum thickness. This criterion was used in selecting samples of approximately optimum thickness for the experiments described in Chapter III.

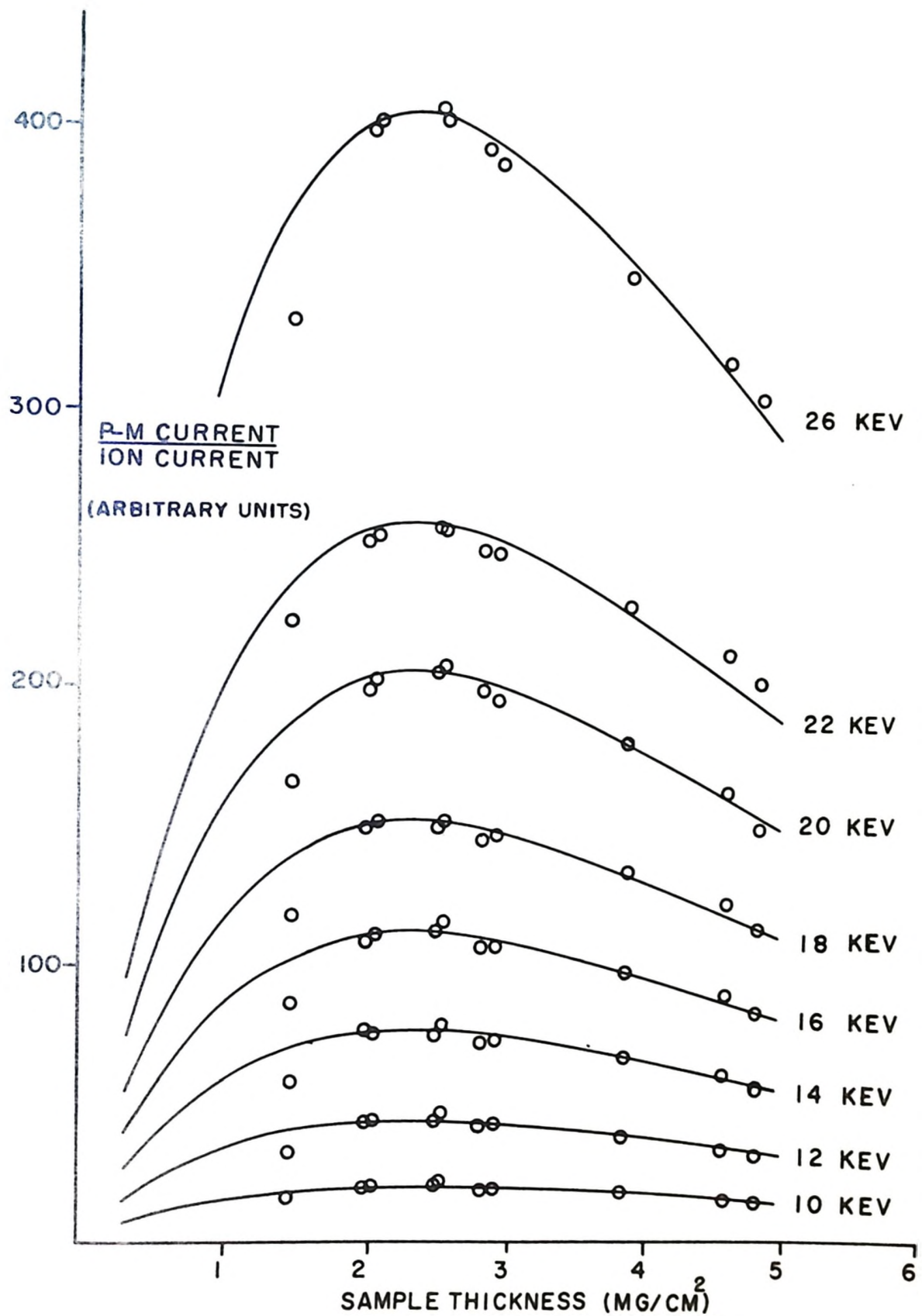
Again it should be emphasised that the foregoing theory is to be regarded as only an approximation because the detailed mechanism by which light is transmitted through the powdered sample has been ignored. More detailed analyses of the optics of powdered materials have been given by Bodó and Hantos (1956), Ivanov (1956) and Gergely (1956).¹

¹Bodó, Z. and Hantos, I. 1956. Acta Phys. Hungar. 5, 295.
 Gergely, G. 1956. Optica Acta (Paris) 3, 184.
 Ivanov, A.P. 1956. Soviet Physics - J.E.T.P. 3, 121.

The author is indebted to Dr. F.R. Lipsett for drawing his attention to these publications.

Fig. 4

Variation of light output with sample thickness.
The circles represent the experimental points and
the solid lines represent equation (10) for various
values of I_0 with $\alpha = 0.7$ and $K = 0.75 \text{ cm}^2/\text{mg}$.



Chapter III

The Effect of Ion Energy and Type of Ion

The experiments described in this chapter were performed on samples of ZnS:Ag (Sylvania Phosphor CR-20) and Zn₂SiO₄:Mn (Sylvania Phosphor 161) to determine how the luminescent efficiency of these phosphors depends on the energy and the nature of the bombarding ions. In all of these experiments, except in the one case indicated, the luminescence was detected by a photomultiplier located on the side of the samples remote from that bombarded by the ions.¹

1. The Form of the Energy Dependence

In the first experiment, a sample of ZnS:Ag was bombarded with K⁺ ions. It was found that the light output was directly proportional to the ion current for a given ion energy. Thus, for each ion energy, it was possible to correct the photomultiplier response to a standard ion current of 10⁻¹³ amp. This corrected photomultiplier

¹In the designation of the different phosphor samples in the diagrams of this chapter, the letter A following the sample number indicates that the sample was of approximately optimum thickness and that the light was measured on the side of the sample remote from that bombarded by ions. The absence of a letter indicates a thick sample, the light from which was detected on the bombarded side.

response is plotted as a function of the ion energy, E , in fig. 5. On a logarithmic scale the curve is linear within the range of ion energies used, and has a gradient, n , of 2.46. Hence the light output, L , varies with the ion energy according to

$$L \propto E^n, \quad (16)$$

where n is approximately 2.5.

Hanle and Rau (1952) found that the luminescent intensity of ZnS:Ag, under bombardment with H_2^+ ions, was directly proportional to the ion energy to within 5 or 6%, for energies in the range 15 to 35 KeV. This contrasts sharply with the result for K^+ ions stated above. In the experiment of Hanle and Rau, the photomultiplier was located on the same side of the phosphor sample as that bombarded by the ions, so that the detected light suffered virtually no optical absorption in the phosphor, whereas in the present experiment the light was detected after transmission through the phosphor layer. In order to be sure that the optical absorption of the phosphor did not change with increasing ion energy, due to a shift in the emission spectrum of the phosphor, a second experiment was performed with the photomultiplier located on the bombarded side of the sample.

The results of the second experiment are shown in fig. 6. When the ratio, L , of the photomultiplier current

to ion current, is plotted against E on a logarithmic scale, the experimental points for ion energies greater than about 17 KeV fall on a straight line of gradient 2.47. This confirms the result of the first experiment, which therefore was not invalidated by any change in the optical absorption of the phosphor.¹ It is to be noted that the experiment described in Chapter II also indicates the absence of any change in the optical absorption of the phosphor with increasing ion energy. Any variation of α in equation (11) would entail a variation of M_{\max} , which is a sensitive function of α for $\alpha = 0.7$. No such variation of M_{\max} is to be seen in fig. 4.

In the second experiment, measurements were extended to lower ion energies than were used in the first experiment. In the curve of L versus E , shown in fig. 6, the experimental points corresponding to ion energies less than about 17 KeV do not fall on the straight line through the higher energy points. It was found, however, that if L was plotted against $(E - 6\text{KeV})$, instead of E , the experimental points for all energies fall on a straight line. This suggests that the variation of the light output with the ion energy is more

¹At this stage of the work it still remained to be shown that there was no shift in the emission spectrum of the phosphor with increasing ion energy. Such a shift would invalidate the conclusions of both the first and the second experiments because of the spectral dependence of the photomultiplier sensitivity. Evidence is presented later in this chapter to show that such a shift does not occur.

accurately represented by

$$L \propto (E-E_0)^n \quad (17)$$

than by the relation (16). The present experiment indicates that for K^+ bombardment of ZnS:Ag, E_0 is about 6 KeV and n about 1.8.

The results of an experiment with K^+ ions on another sample of ZnS:Ag, together with a few points for Na^+ ions, are shown in fig. 7.

2. Variation with the Nature of the Bombarding Ions

In order to determine how the quantities E_0 and n vary with the nature of the bombarding ions, a series of experiments was performed in which ZnS:Ag and $Zn_2SiO_4:Mn$ were bombarded with Li^{7+} , Na^+ , K^+ , Rb^+ and A^+ ions, and ZnS:Ag with H_2^+ ions. To eliminate any possible sample to sample variation of E_0 and n , a single sample of ZnS:Ag (sample 10A) and a single sample of $Zn_2SiO_4:Mn$ (sample 9A) were used throughout this series of experiments.

In each experiment the procedure adopted was to determine the photomultiplier current for a number of different values of the ion current, at a given ion energy. For each ion energy, the photomultiplier current was plotted as a function of the ion current. The gradients, L , of the lines so obtained, were then plotted as a function of the ion energy E . The results of this series of experiments

are shown in figs. 9-24.

An example of the variation of photomultiplier current with ion current is shown for the case of Na^+ ions on ZnS:Ag in fig. 8. Note that the value of L is approximately doubled when the ion energy is increased from about 16 to about 20 KeV. This clearly shows the non-linear character of the relationship between L and E .

In the experiment with Li^{7+} ions on ZnS:Ag , some measurements were made with an optical interference filter interposed between the phosphor sample and the photomultiplier. The transmission spectrum of the filter is represented by the curve C in fig. 3. The peak emission wavelength of the phosphor, as given in the Sylvania catalogue, lies close to the wavelength of maximum transmission of the filter. Furthermore, the width of the emission peak at half-intensity is about the same as the half-intensity width of the transmission peak of the filter. The two peaks are thus approximately matched. A shift in the emission spectrum of the phosphor (from its position as given in the catalogue) would therefore be accompanied by a change in the effective transmission of the filter. Hence, if such a shift occurred with increasing ion energy, the relationship observed between L and E with the filter in position would differ from that observed with no filter. No such difference was in fact observed. As is shown in

fig. 9, when the values of L obtained with the filter in position were multiplied by a constant factor of 6.71, the experimental points fell accurately on the line obtained with no filter. Hence there is no shift in the emission spectrum of the phosphor, and the values of L determined in these experiments truly represent the relative intensity of luminescence of the phosphor.¹

The value of the factor 6.71 is somewhat higher than would be expected on the basis of the spectra shown in fig. 3. This is attributed to the fact that the distance between the phosphor sample and the photomultiplier had to be increased in order to accommodate the filter.

The results shown in fig. 13 for K^+ ions on ZnS:Ag, indicate a value of about 4 KeV for E_0 . This does not agree with the previous value quoted for K^+ ions on other samples (see figs. 6 and 7). Because of this disagreement, a second experiment with K^+ ions on sample 10A was performed. The results of both experiments are shown in fig. 13, from which it can be seen that consistent results as regards both E_0 and n were obtained for sample 10A. In the experiments on samples 10 and 1A (figs. 6 and 7), the lowest K^+ ion energy used was $E = 9.2$ KeV. In fig. 13, the solid line through the experimental points representing L versus $(E - 6\text{KeV})$ has been terminated at this value of E . It is seen that for values of E in excess of 9.2 KeV, the experi-

¹A full spectral analysis was not feasible because of the low intensity of the emission. This intensity could only be sufficiently increased at the expense of seriously deteriorating the phosphor sample.

mental points fall approximately on this line, so that in this part of the energy range the results of this experiment also appear consistent with a value of 6 KeV for E_0 . Hence there is in fact no essential disagreement between the experiments on the different samples. However, the five points corresponding to $E < 9.2$ KeV in fig. 13, are obviously inconsistent with $E_0 = 6$ KeV. It is clear that an accurate determination of E_0 requires the measurements to be extended to as low ion energies as possible. Hence, in the experiments on samples 10A (ZnS:Ag) and 9A (Zn₂SiO₄:Mn), the value of E was decreased to the point where the photomultiplier response became comparable with the dark current. Accurate values of L are, of course, unobtainable beyond this point. In order to be sure that the value obtained for E_0 was not merely a function of the lowest value of E used, in each one of the experiments on samples 10A and 9A the experimental points were plotted for several values of E_0 . The limiting lines, in which curvature was just detectable, were taken to indicate the experimental limits between which the value of E_0 lay. These are the limits assigned to E_0 in table I below. The limits assigned to n are the gradients of the limiting lines.

The results of the experiment with H_2^+ ions on ZnS:Ag are plotted on a linear scale in fig. 19, from

which it can be seen that the relationship between L and E is approximately linear, but has a threshold of some 4 KeV. This is in approximate agreement with the results of Hanle and Rau (1952). The values of E_0 and n that are quoted for H_2^+ ions in table I were obtained from a logarithmic plot, in the same manner as were the values for the other ions.

In the case of $Zn_2SiO_4:Mn$, the only bombarding ion for which E_0 was distinguishable from zero was Li^{7+} . The experiment was therefore repeated with Li^{7+} ions. The results of this second experiment were in agreement with those of the first.

Table I

ION	ZnS:Ag		Zn ₂ SiO ₄ :Mn	
	E_0 (KeV)	n	E_0 (KeV)	n
H_2^+	3.5 ± 0.5	1.11 ± 0.06		
Li^{7+}	4.0 ± 0.5	1.67 ± 0.10	2.5 ± 0.5	1.29 ± 0.07
Na^+	3.5 ± 0.5	3.26 ± 0.20	<1.0	1.79, 1.64
K^+	4.0 ± 0.5	2.35 ± 0.13	<1.0	1.74, 1.60
A^+	2.0 ± 1.0	3.11 ± 0.27	<2.0	1.81, 1.47
Rb^+	1.8 ± 1.8	3.89 ± 0.60	<1.0	1.90, 1.76

The results given in table I are shown graphically as functions of the mass of the bombarding ions in figs. 20-22.

In fig. 23 and 24, L is plotted as a function of ion mass for three different ion energies. The points at zero mass represent results for electrons. In the case of

$\text{Zn}_2\text{SiO}_4:\text{Mn}$, it can be seen that the light output falls off rapidly with increasing mass of the bombarding particles in a fairly regular manner. For $\text{ZnS}:\text{Ag}$, there is an irregularity in the curves in the region of mass 40. In comparing the curves of L versus ion mass for $\text{ZnS}:\text{Ag}$ with those for $\text{Zn}_2\text{SiO}_4:\text{Mn}$, it should be noted that no correction has been made for the spectral change in the sensitivity of the photomultiplier from one phosphor to another.

3. The Effect of Deterioration

In the introduction to this thesis, reference was made to work demonstrating the deterioration of the luminescent efficiency of phosphors under prolonged ion bombardment. This deterioration effect is especially important in the case of $\text{ZnS}:\text{Ag}$. Martin (1957) found that this phosphor deteriorated more rapidly under H_2^+ ion bombardment than any of the other phosphors that he studied (including $\text{Zn}_2\text{SiO}_4:\text{Mn}$). It is therefore very important to show that, during the course of the series of experiments on sample 10A of $\text{ZnS}:\text{Ag}$ described above, no appreciable deterioration of the phosphor occurred. This was shown by the three experiments described below.

(i) The experiment with Li^{7+} ions, which was the first of the series, was repeated at the conclusion of the series, and the same L versus E curve was obtained.

(ii) After the conclusion of the series, the light

output of sample 10A was compared with that of a fresh sample of ZnS:Ag under bombardment with A^+ ions at three different energies. The ratio, L_1/L_2 , of the light output of sample 10A to that of the fresh sample is given for each ion energy in table II.

Table II

Ion energy (KeV)	L_1/L_2
10	1.16
15	1.13
20	1.17

It is seen that this ratio is independent of the ion energy. It was therefore concluded that the form of the L versus E curve was not affected by the ion bombardment to which sample 10A had previously been subjected. Actually, the value of L for sample 10A was slightly greater than that for the fresh sample at each energy. This difference is attributed to a difference in sample thickness (see Chapter II).

(iii) An experiment was performed in which the rate of deterioration of ZnS:Ag under bombardment with 15 KeV A^+ ions was determined. The results of this experiment are shown in fig. 25, in which the ratio, L_0/L , of the initial light output to that after time t, is plotted against N, the number of ions per unit area that have impinged on the sample during time t. The experimental points lie on the line

$$I_0/L = 1+cN, \quad (18)$$

where c is a constant. This equation is in agreement with the law found by Hanle and Rau (1952) and confirmed by Martin (1957). Measurement of the gradient of the line in fig. 25 gives for the deterioration constant c the value $1.04 \times 10^{-11} \text{ cm}^2$. This value agrees approximately with that found by Hanle and Rau (1952) for A^+ bombardment of ZnS:Ag, namely $0.95 \times 10^{-11} \text{ cm}^2$.

If it is assumed that all the ions, used in the series of experiments on sample 10A, penetrated the phosphor to the same depth, and that the value of c for all these ions is about 10^{-11} cm^2 , then the deterioration of sample 10A can be estimated by summing the ion flux to which the sample was subjected during this series, account being taken of the fact that the samples were kept in motion during bombardment. A deterioration of about 6.5% was estimated in this way. Martin (1957) has shown that the value of c is approximately independent of the energy of the ions. However, the depth of penetration of the ions into the phosphor in fact depends on the energy and mass of the ions, neither of which was constant throughout this series of experiments. Young (1955) has shown that his results are consistent with the assumption that, when a phosphor is bombarded with ions of a given energy, the phosphor is uniformly deteriorated throughout the depth

of penetration of the ions. If this is so, then it follows that the 6.5%, estimated above, in fact represents the maximum deterioration, present near the surface of the phosphor in a region penetrated by all the ions. In deeper lying regions, penetrated only by ions of higher energy or lower mass, the deterioration will be less than 6.5%. Hence, in order to correct the graphs shown in figs. 9-24 for the effect of deterioration, the value of L corresponding to each point of a given graph must be increased by an amount between 0 and 6.5%, the percentage correction being greater for the lower energy points. The maximum possible change in the form of the L versus E curve is obtained by applying the maximum correction of 6.5% to the lowest energy point, zero correction to the highest energy point, and intermediate corrections to the other points according to their energies. When this was done, it was found that the mean values obtained for n and E_0 in no case lay outside the experimental limits stated in table I.

4. Deterioration with Very Low Energy Ions

In order to obtain information concerning the physical nature of the constant E_0 , a further experiment was performed on sample 10 (ZnS:Ag) in which a region of the phosphor was subjected to prolonged bombardment with a high intensity beam (about 1.3×10^{-10} amp/cm²) of 6 KeV

K^+ ions. A small light output, which decreased in accordance with equation (18), was obtained. When the light output had fallen by 85%, the phosphor sample was removed from the ion beam. The beam intensity was then decreased to about 5×10^{-13} amp/cm² (at which intensity the deterioration effect is negligible) and the ion energy increased to 12 KeV. The response of all regions of the phosphor sample to 12 KeV K^+ ions was then determined by slowly passing the sample across the path of the beam. As the sample crossed the beam the photomultiplier output was displayed as a peak on the recorder chart in the usual way (see Chapter I, section 7). There was, however, a narrow trough in the middle of the peak, corresponding to the light from that region of the phosphor deteriorated by the 6 KeV ions. The depth of the trough was approximately 83% of the peak height. This value could not be determined with very high accuracy because the dimensions of the cross section of the deteriorating beam were the same as those of the 12 KeV beam. Minimum light output under the 12 KeV bombardment was there-obtained for only one position of the sample, so that the trough in the peak appeared to have a sharp point at its base. The sample was passed slowly across the beam several times, and the trough depths obtained varied by several percent of the peak height. The 83% quoted above was the maximum value obtained.

The implications of this experiment will be discussed in the next chapter.

Fig. 5

The photomultiplier response, corrected to a standard ion current of 10^{-13} amps, as a function of ion energy for K^+ ion bombardment of a sample of ZnS:Ag.

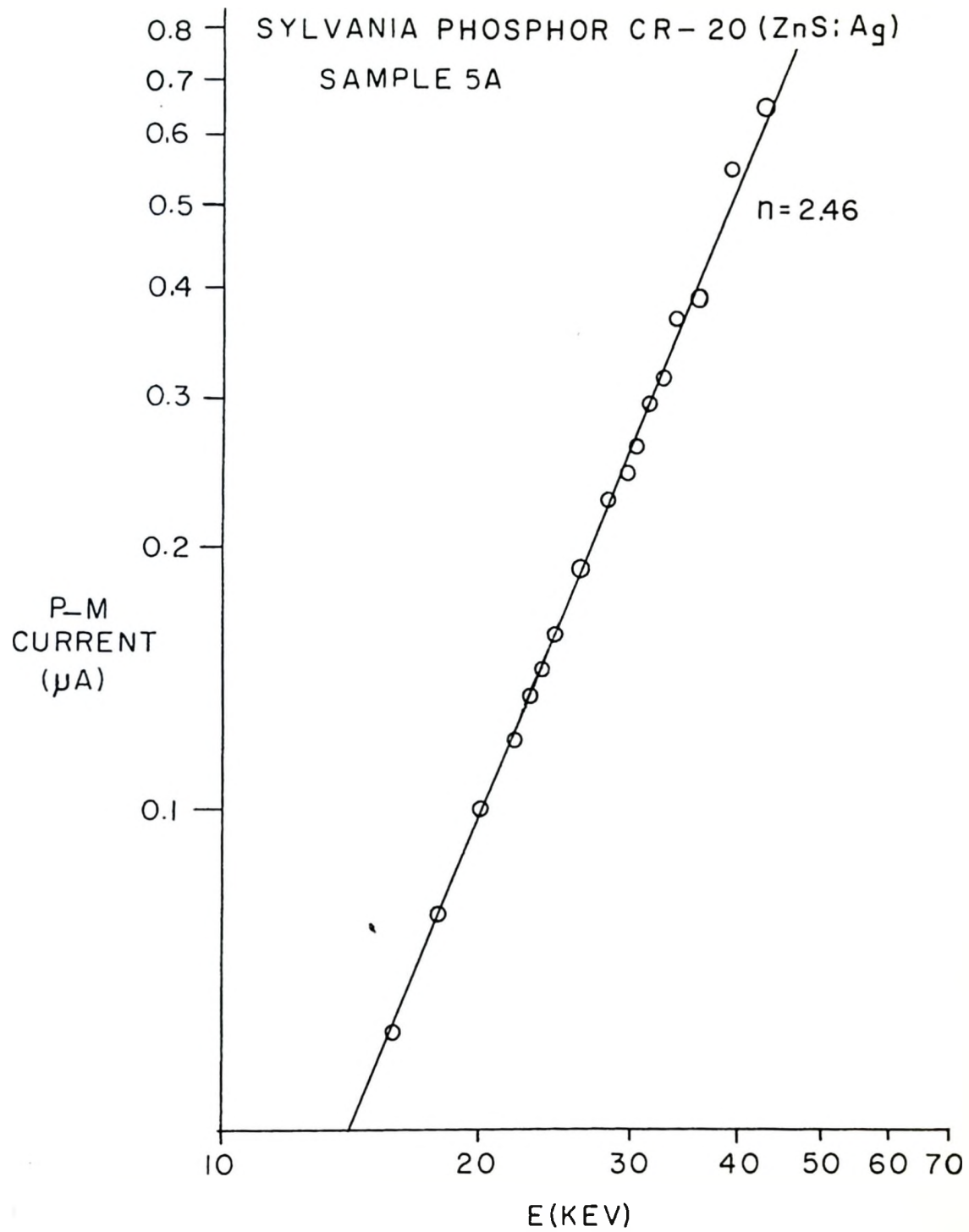


Fig. 6

L versus E and L versus (E - 6 KeV) for K⁺ ion bombardment of a sample of ZnS:Ag (light detected from bombarded side of sample).

SYLVANIA PHOSPHOR CR-20 (ZnS:Ag)
SAMPLE 10

○ 20 DEC. '56

△ 9 JAN '57

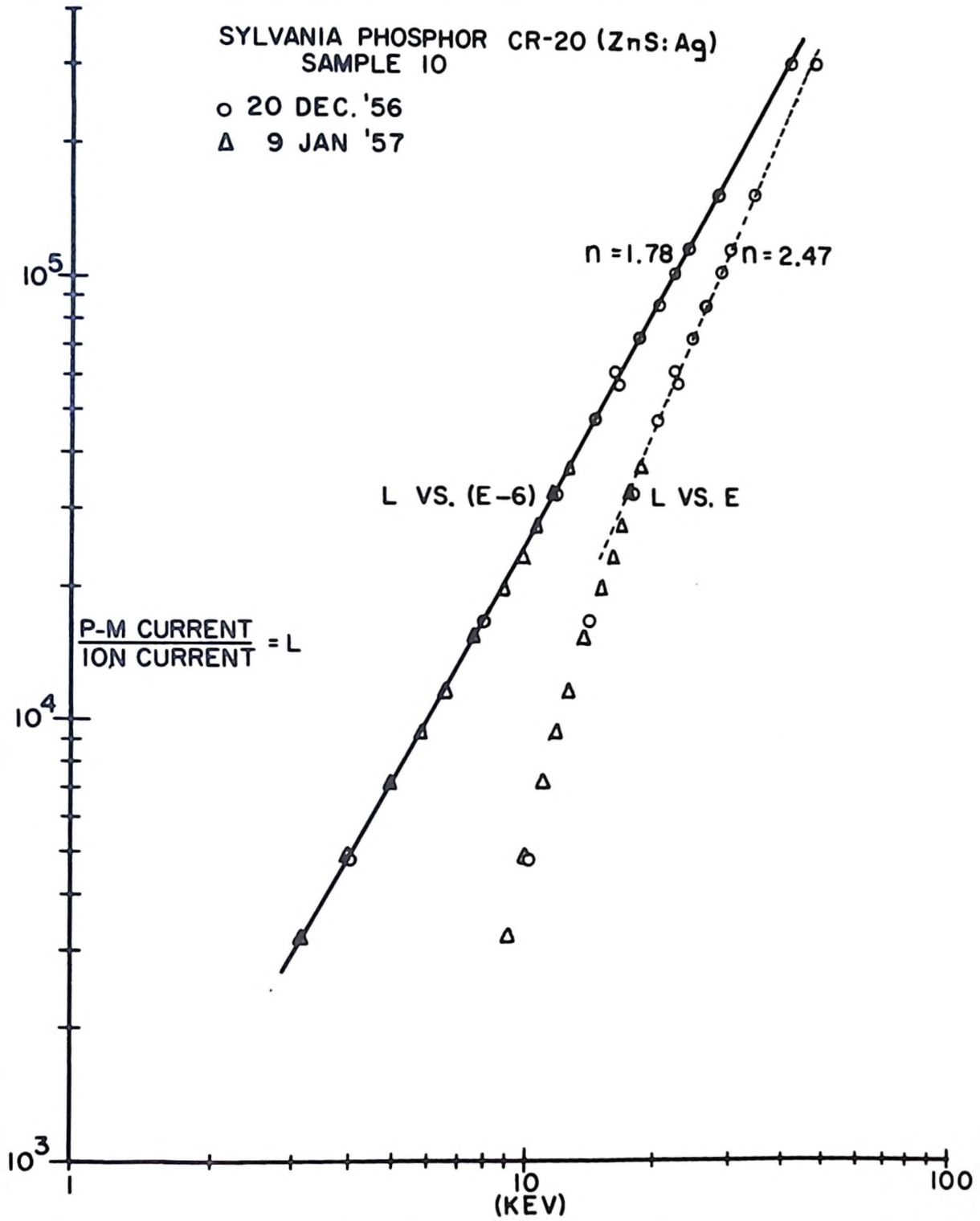


Fig. 7

L versus E and $(E - 6 \text{ KeV})$ for K^+ ions and L
versus E and $(E - 3 \text{ KeV})$ for Na^+ ions on ZnS:Ag .

SYLVANIA PHOSPHOR CR-20 (ZnS:Ag)
SAMPLE 1A

○ K⁺ IONS
△ Na⁺ IONS

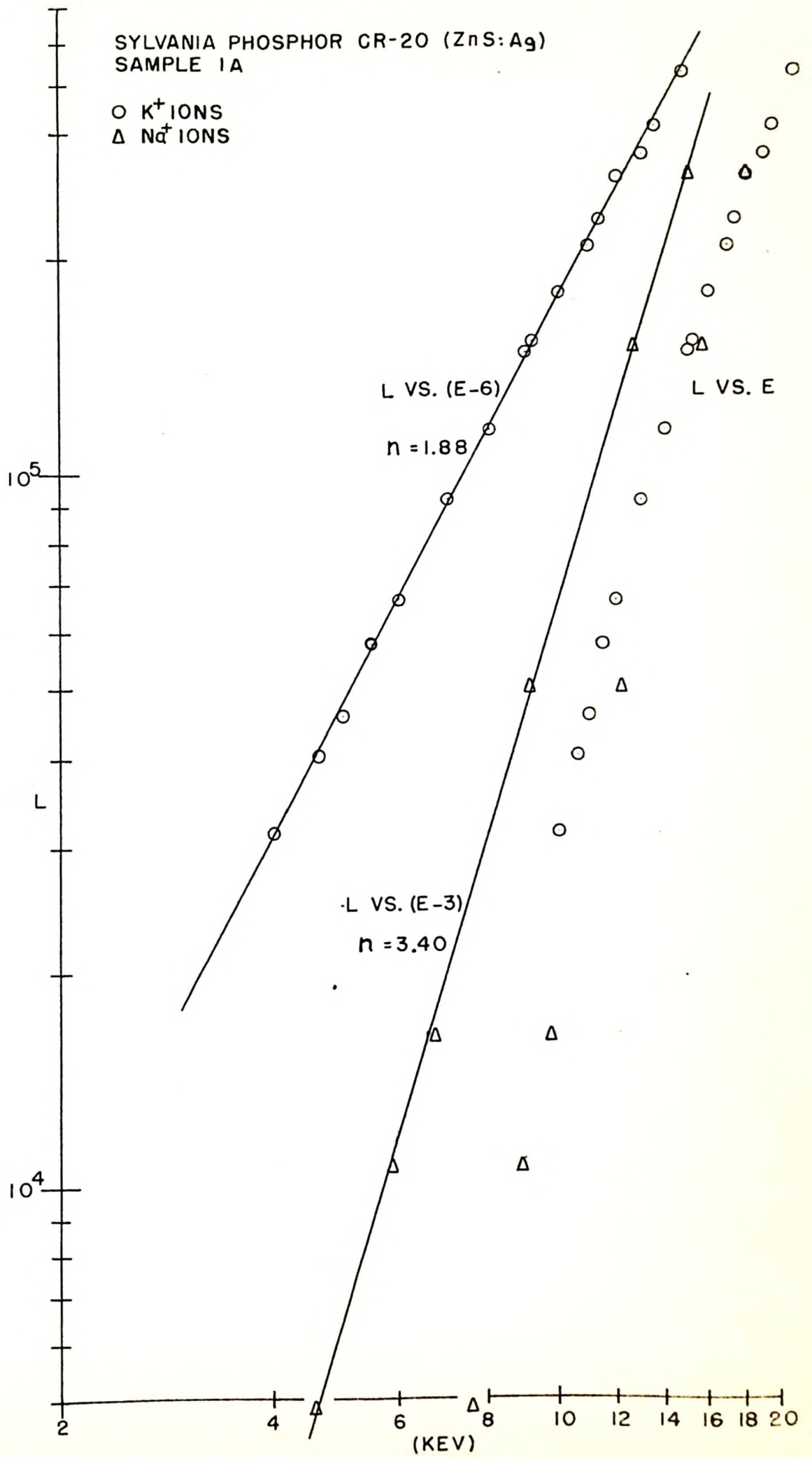


Fig. 8

Variation of photomultiplier response with ion current at two different ion energies.

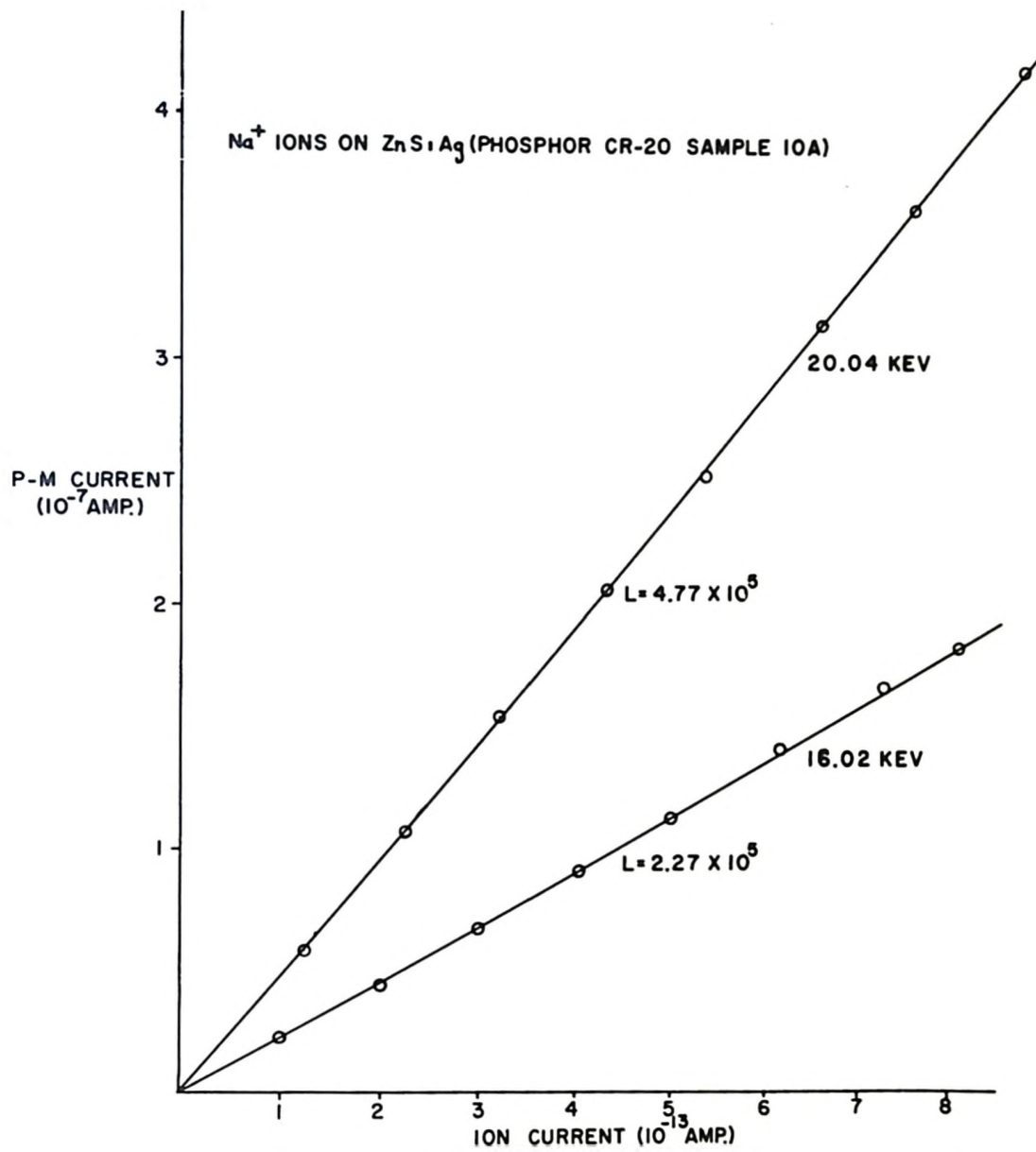
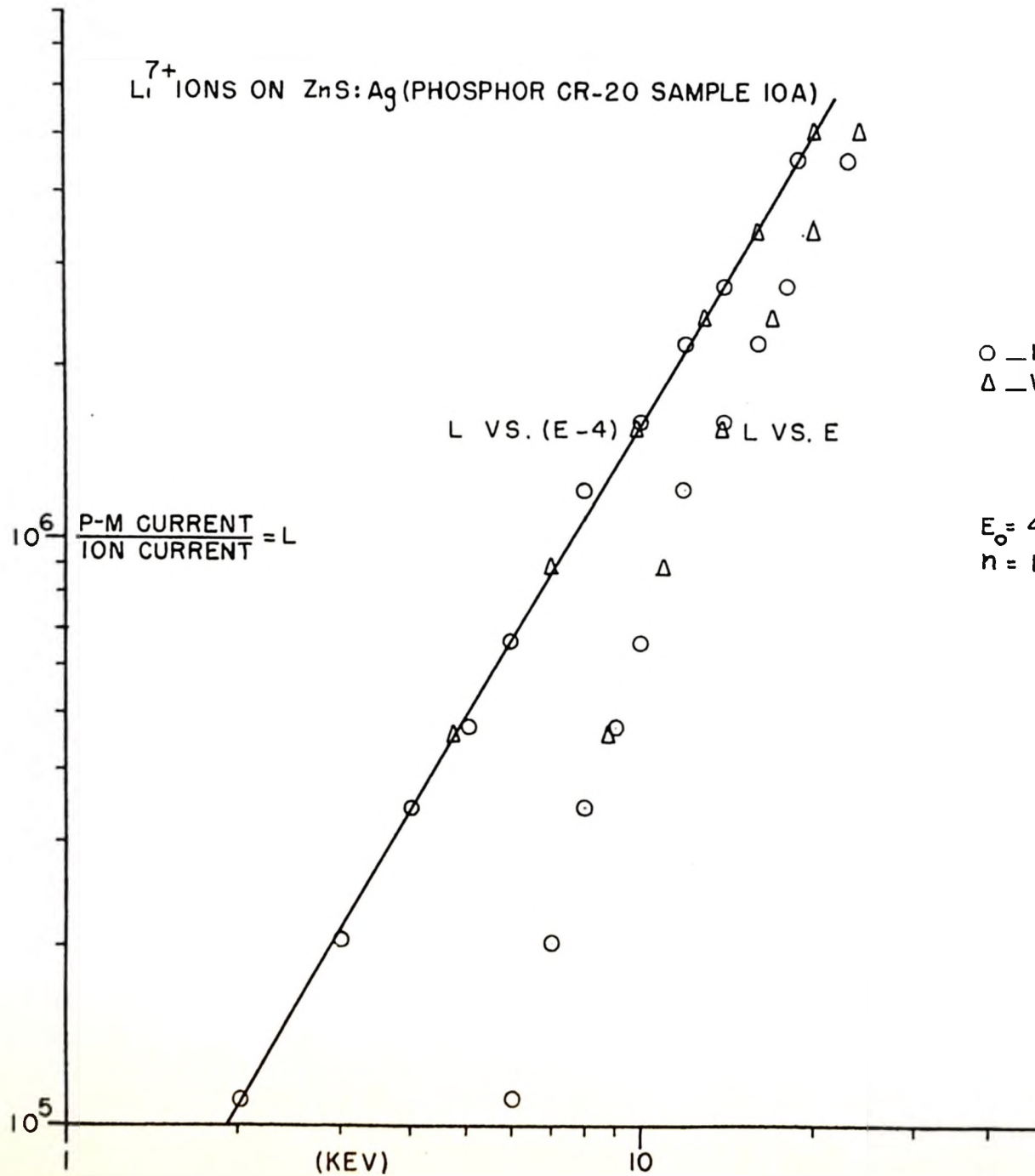


Fig. 9

L versus E and $(E - 4 \text{ KeV})$ for Li^{7+} ions on ZnS:Ag .
The points represented by the triangles were obtained with an optical interference filter interposed between the phosphor sample and the photomultiplier. The transmission spectrum of the filter is represented by the curve C in fig. 3.

Li^{7+} IONS ON ZnS:Ag (PHOSPHOR CR-20 SAMPLE 10A)



○ _ NO FILTER
△ _ WITH FILTER, $L \times 6.71$

$E_0 = 4.0 \pm 0.5$ KEV
 $n = 1.67 \pm 0.1$

Fig. 10

L versus E and (E - 2.5 KeV) for Li^{7+} ions on $\text{Zn}_2\text{SiO}_4:\text{Mn}$.

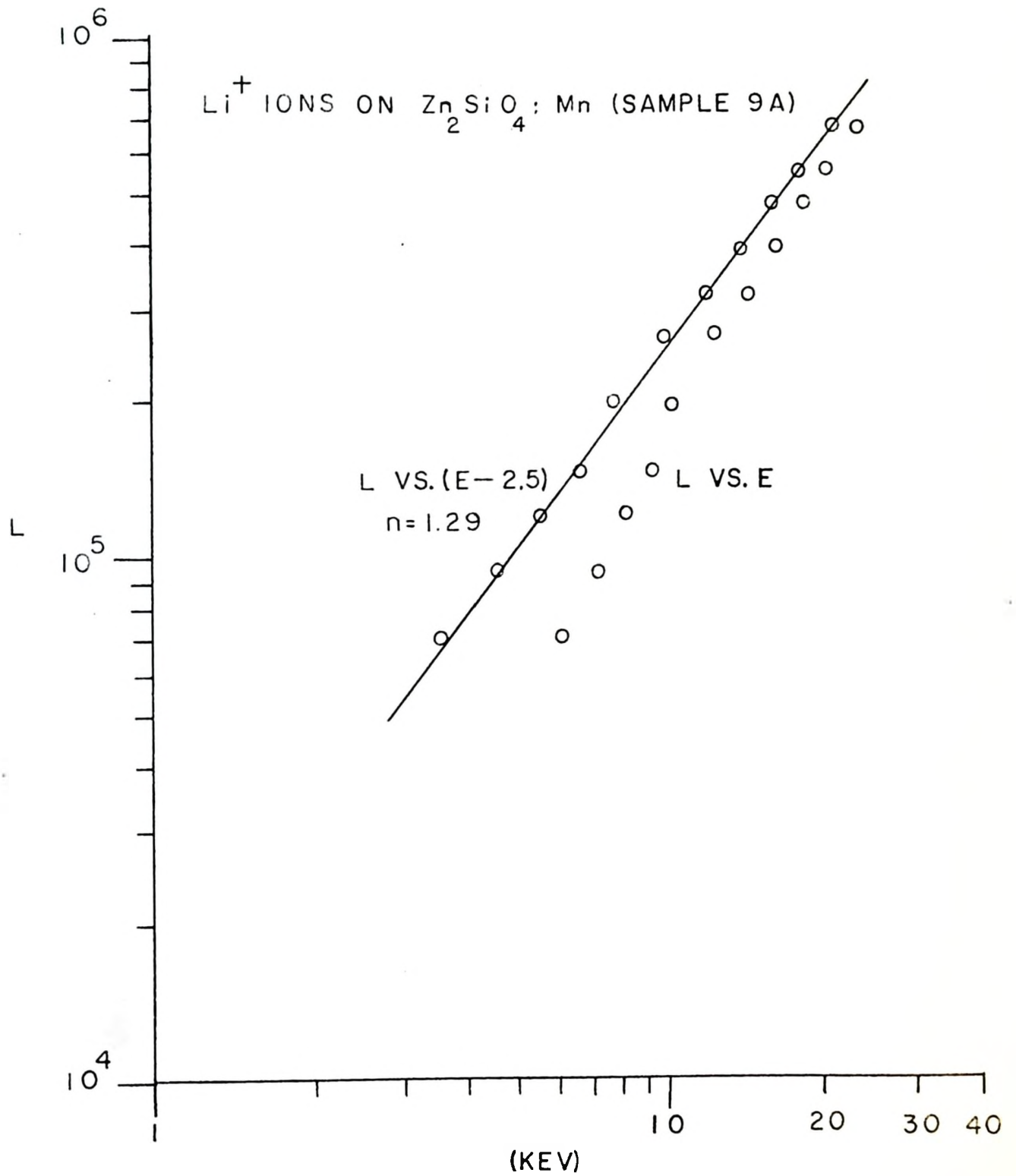


Fig. 11

L versus E and (E - 3.5 KeV) for Na⁺ ions on ZnS:Ag.

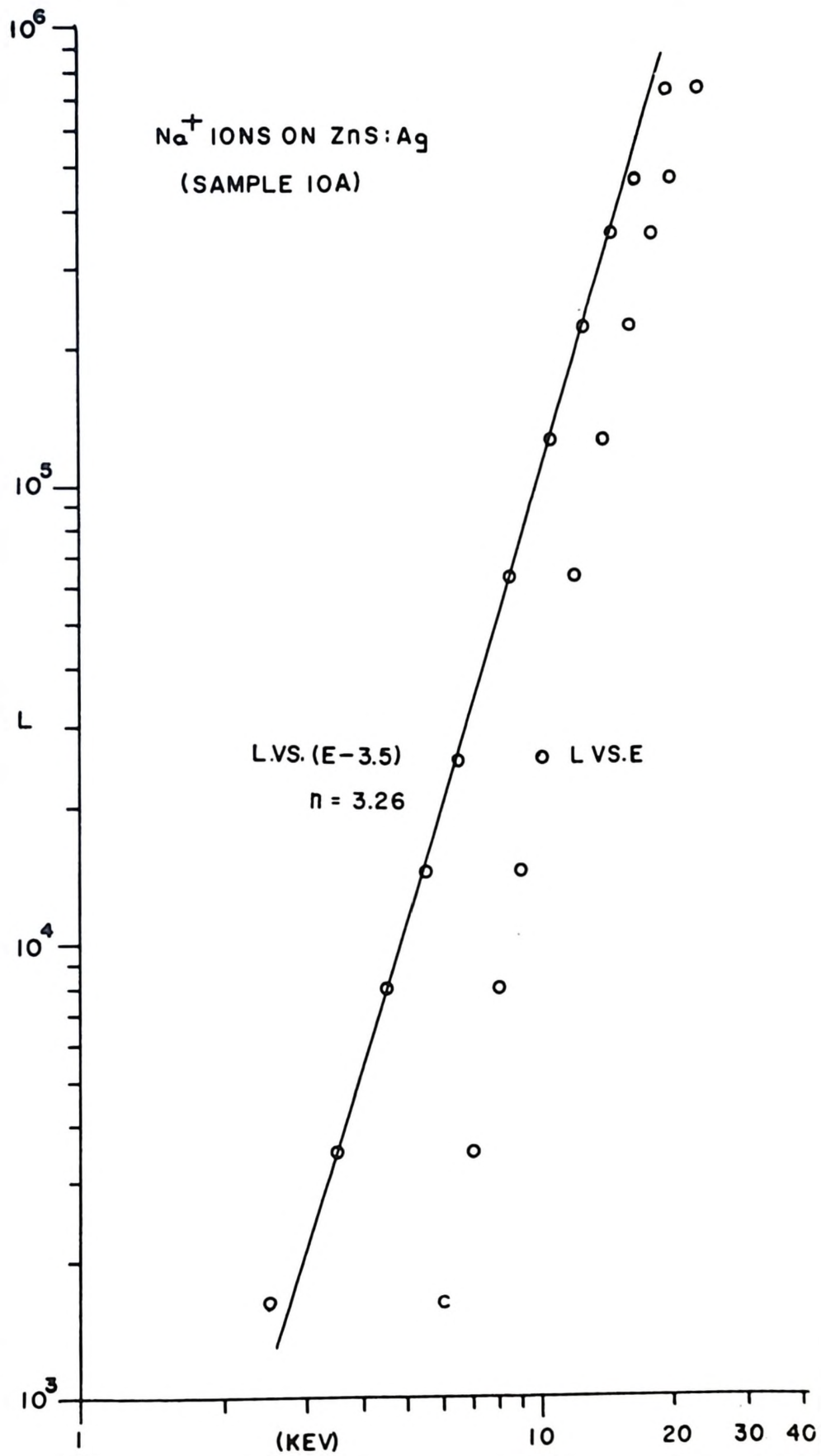


Fig. 12

L versus E for Na⁺ ions on Zn₂SiO₄:Mn.

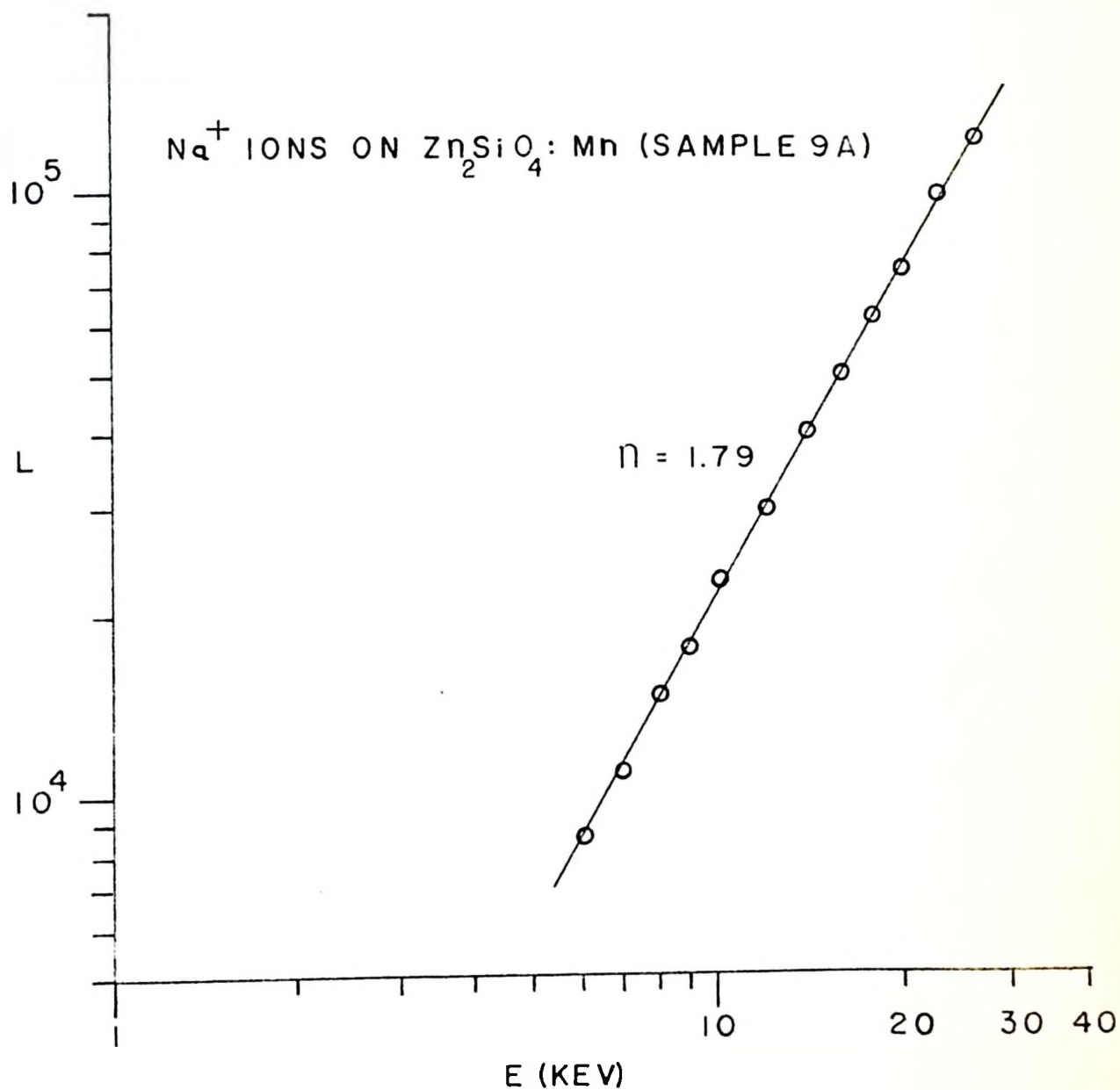


Fig. 13

L versus E, (E - 4 KeV) and (E - 6 KeV) for K^+ ions on ZnS:Ag. The points represented by the circles were obtained in one experiment and those represented by the triangles were obtained in a second experiment performed two days later.

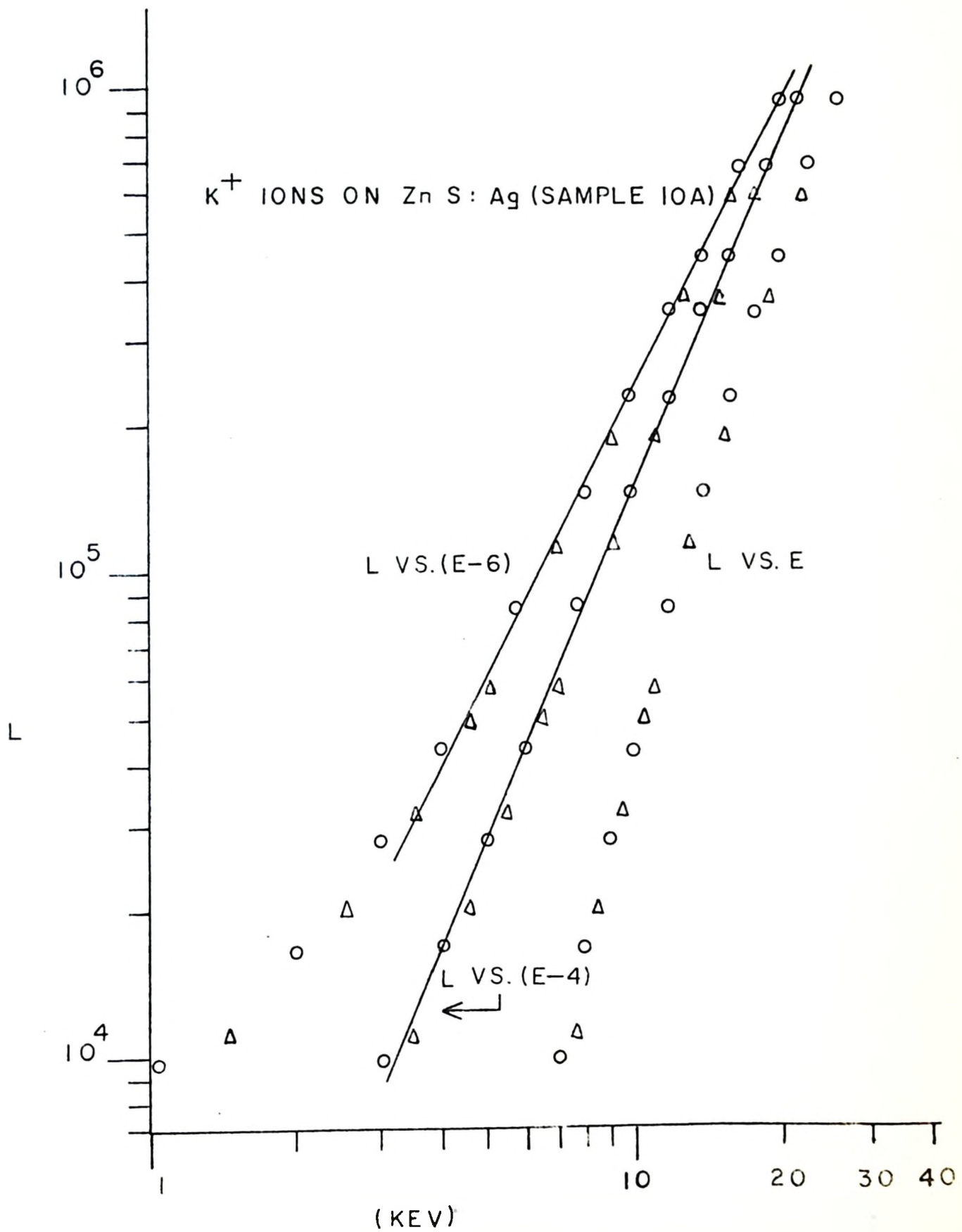


Fig. 14

L versus E for K^+ ions on $Zn_2SiO_4:Mn$. The points represented by the circles were obtained in one experiment and those represented by the triangles were obtained in a second experiment performed two days later.

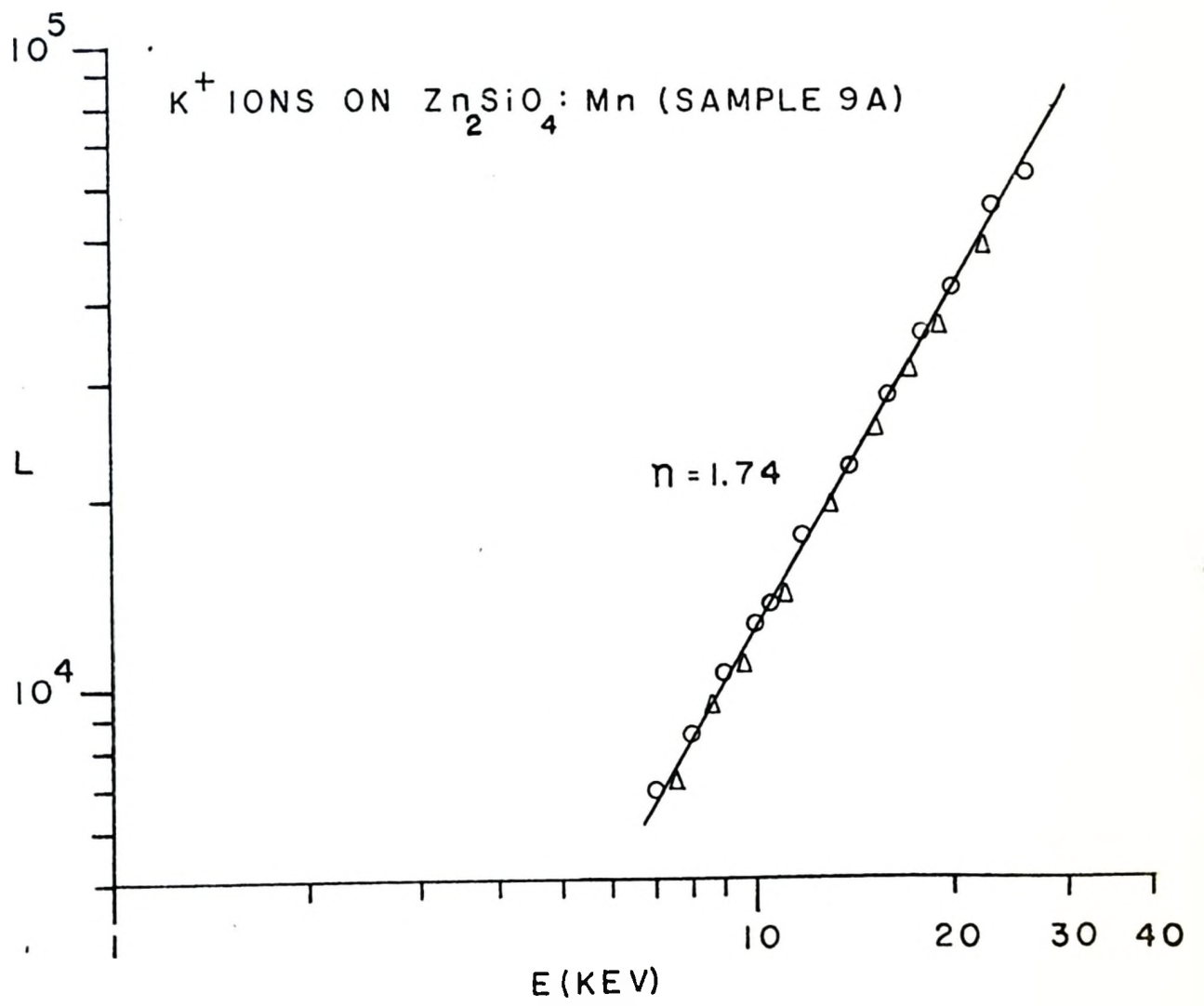


Fig. 15

L versus E and $(E - 3.5 \text{ KeV})$ for Rb^+ ions on ZnS:Ag .

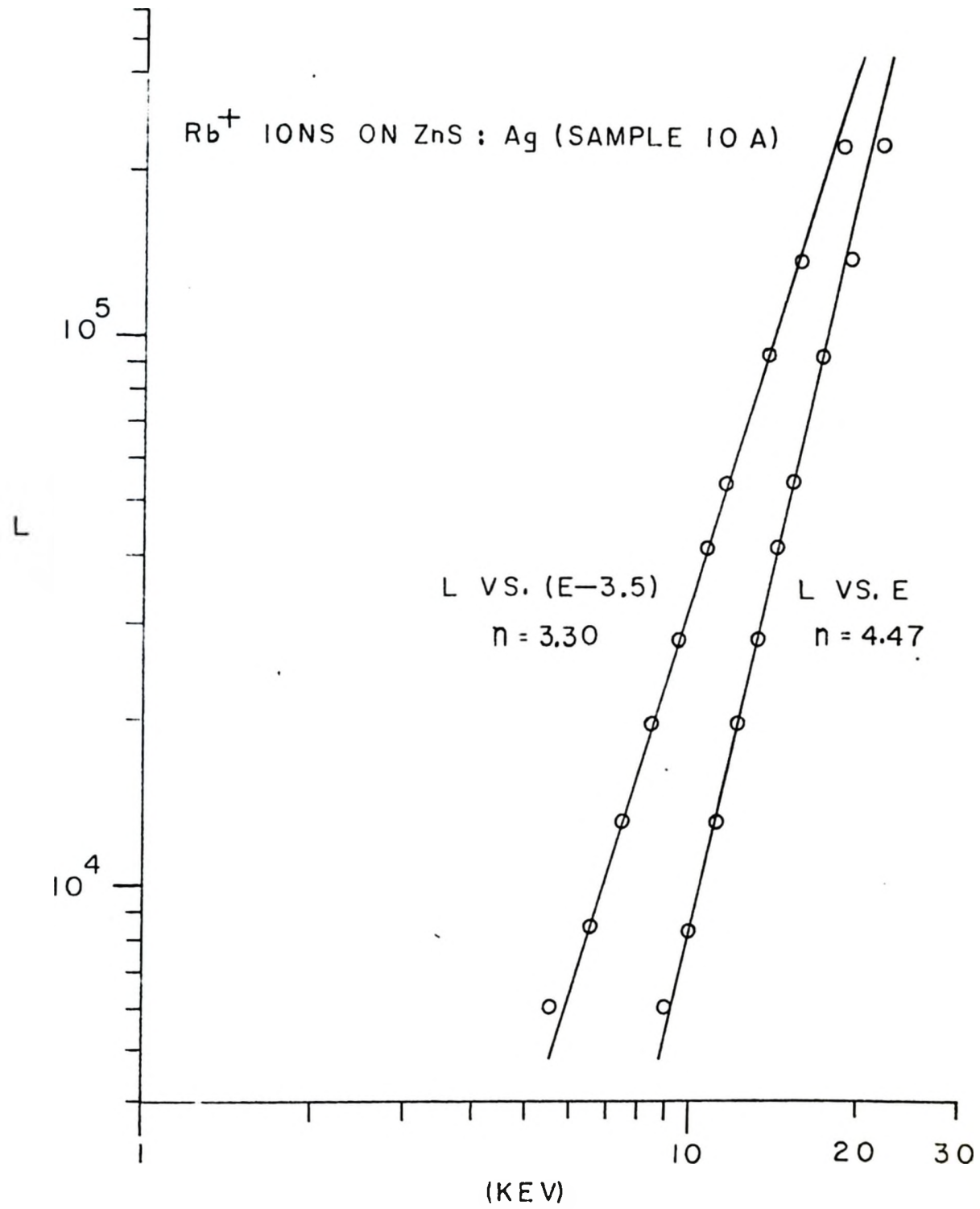


Fig. 16

L versus E for Rb^+ ions on $\text{Zn}_2\text{SiO}_4:\text{Mn}$.

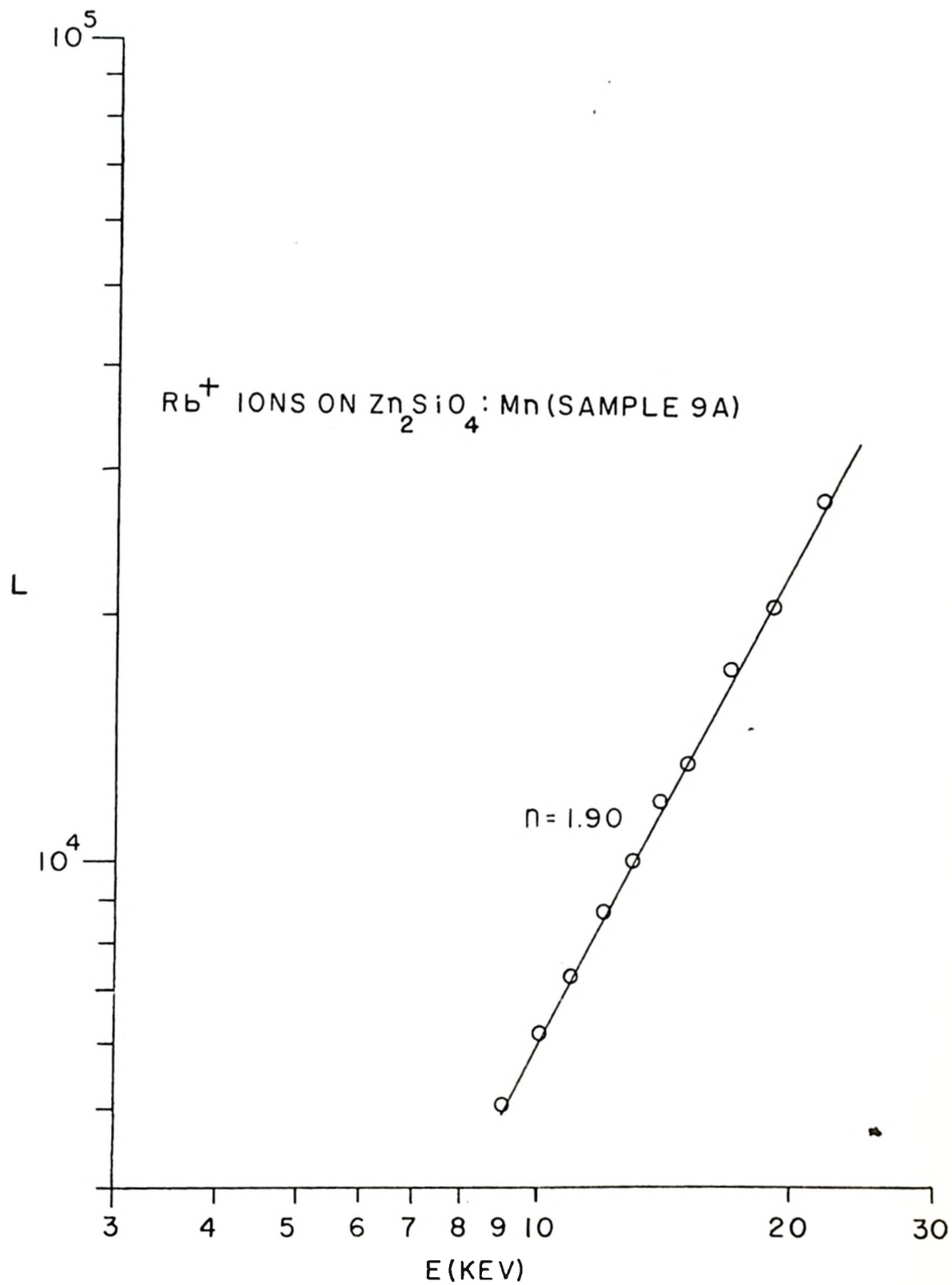


Fig. 17

L versus E and (E - 2 KeV) for A⁺ ions on ZnS:Ag.

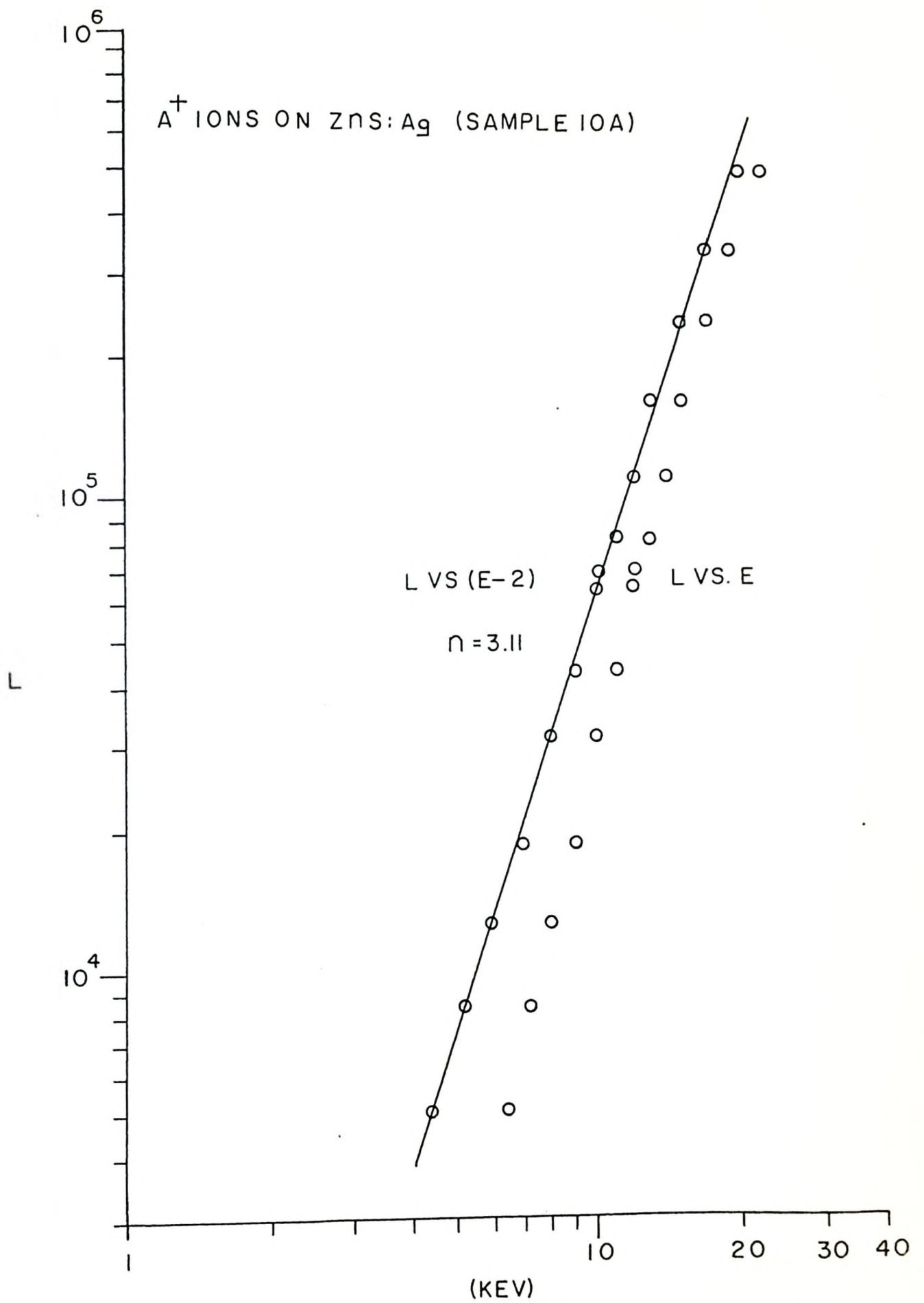


Fig. 18

L versus E for A^+ ions on $Zn_2SiO_4:Mn$.

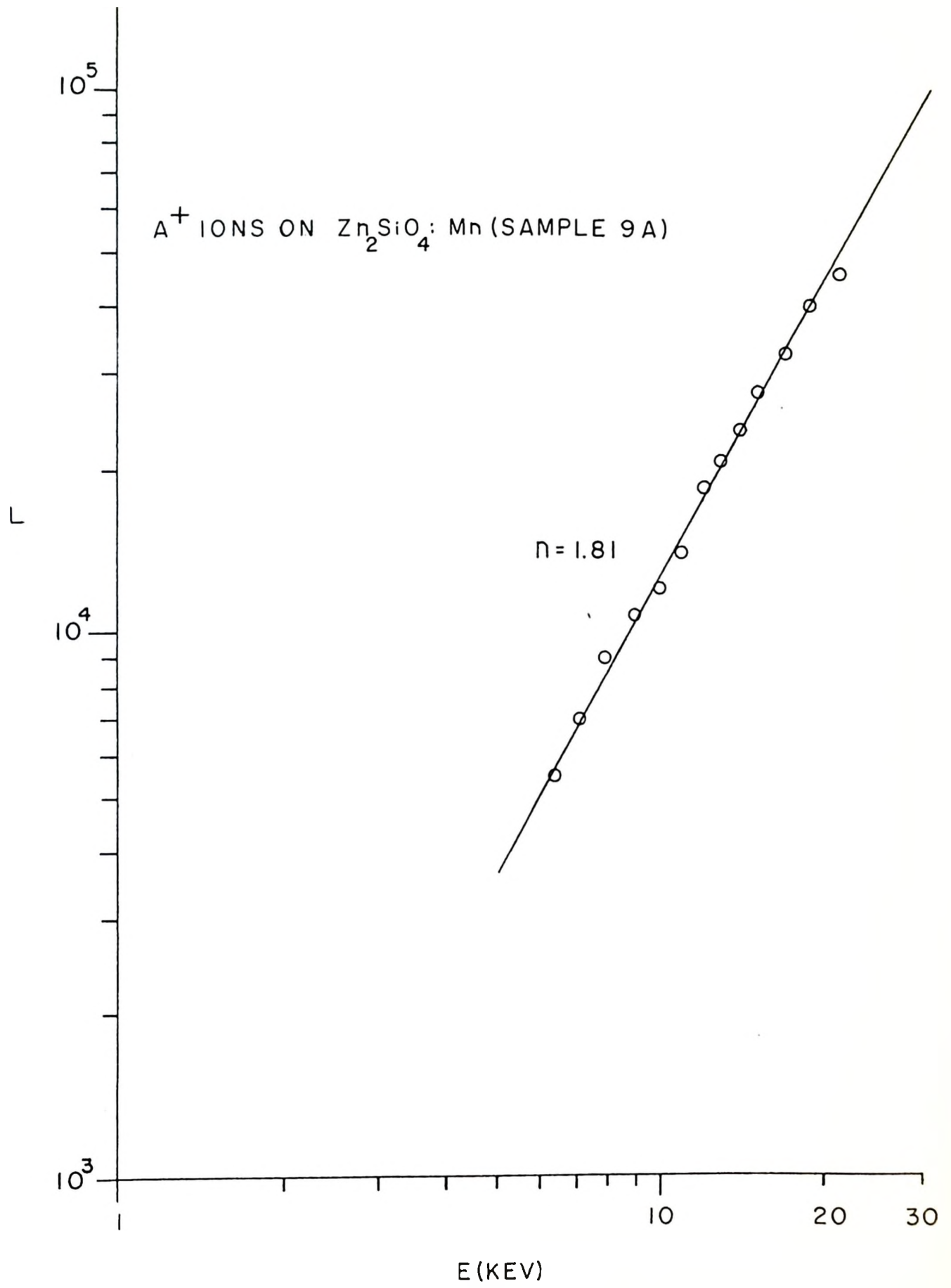


Fig. 19

L versus E for H_2^+ ions on ZnS:Ag.

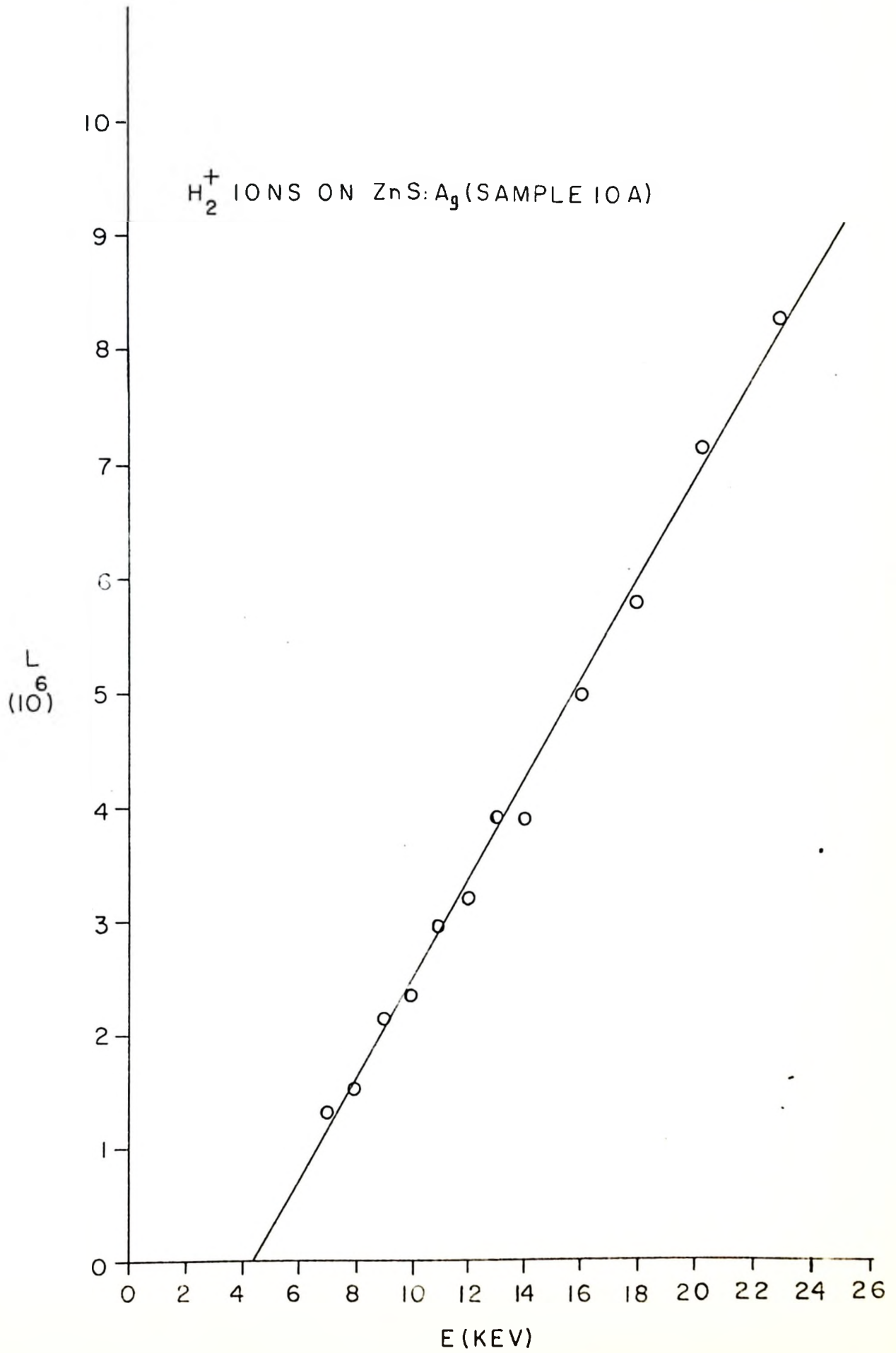
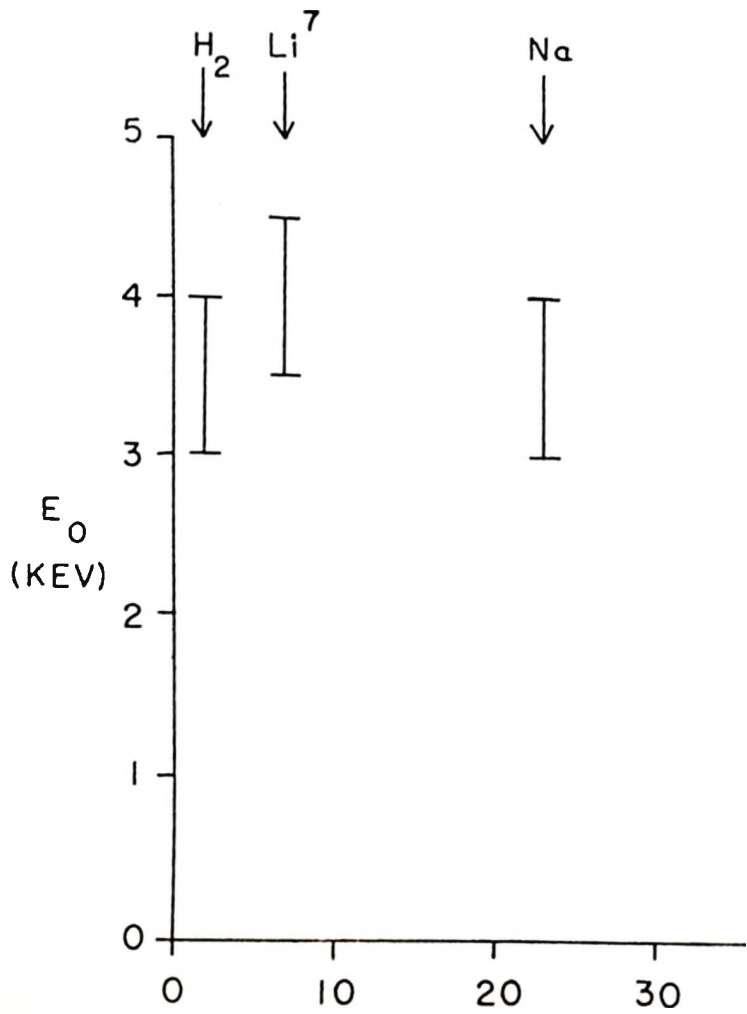


Fig. 20

E_0 as a function of ion mass for ZnS:Ag.



ZnS : Ag

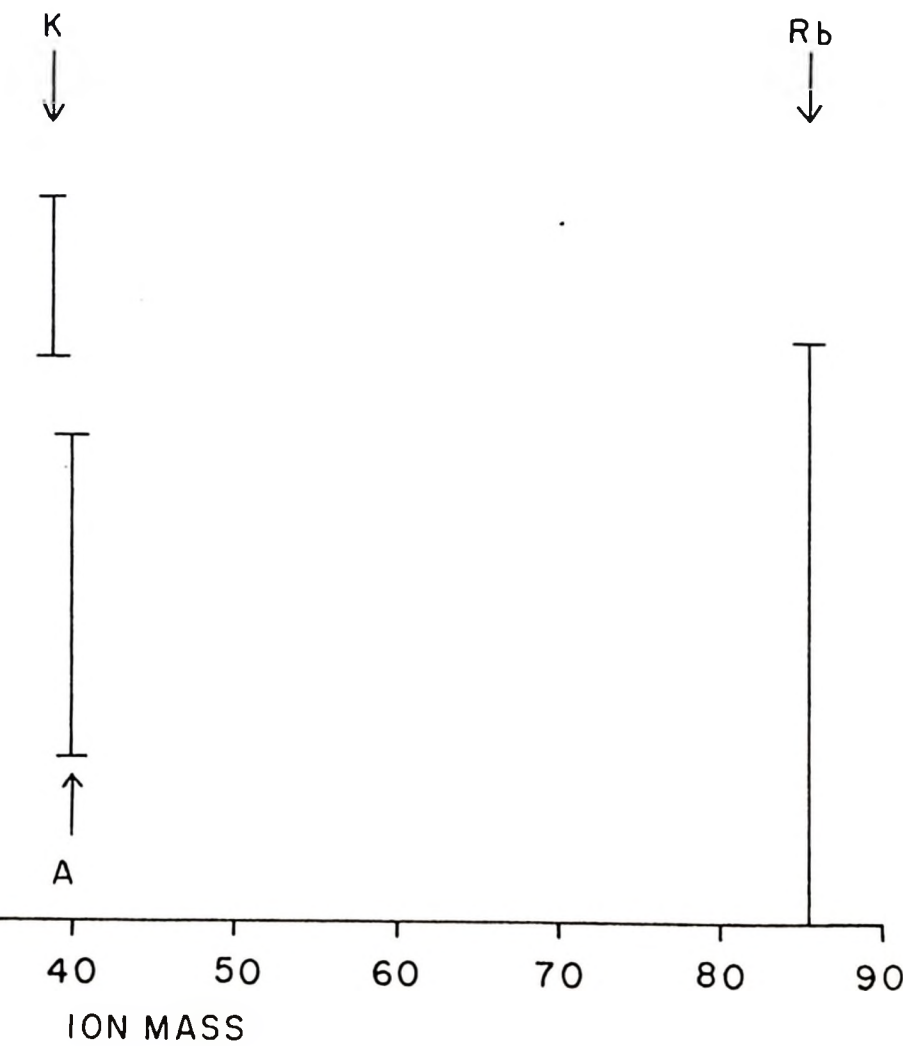
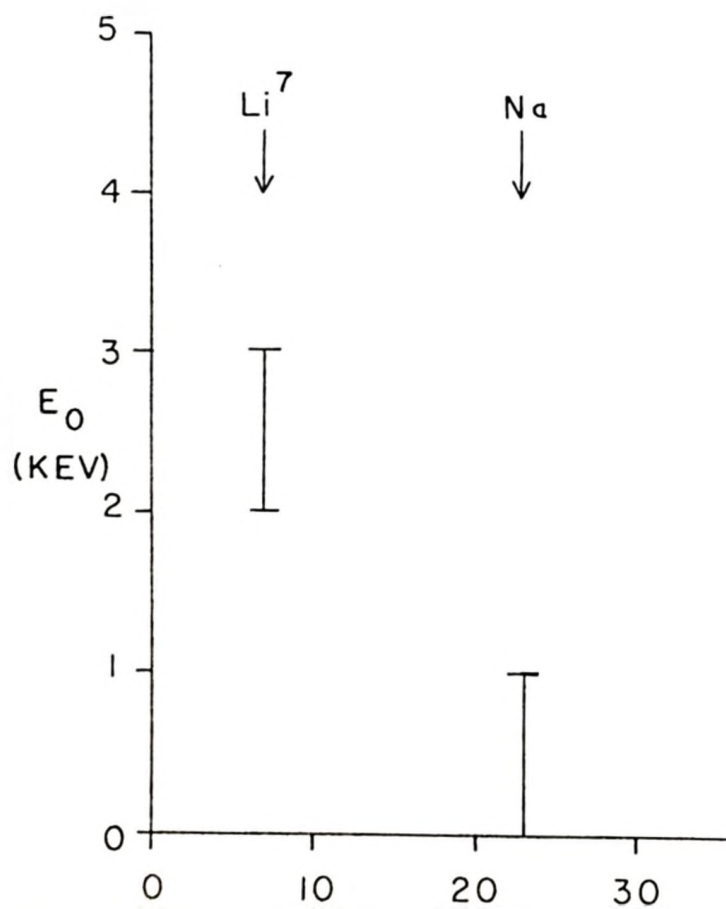


Fig. 21

E_0 as a function of ion mass for $Zn_2SiO_4:Mn$.



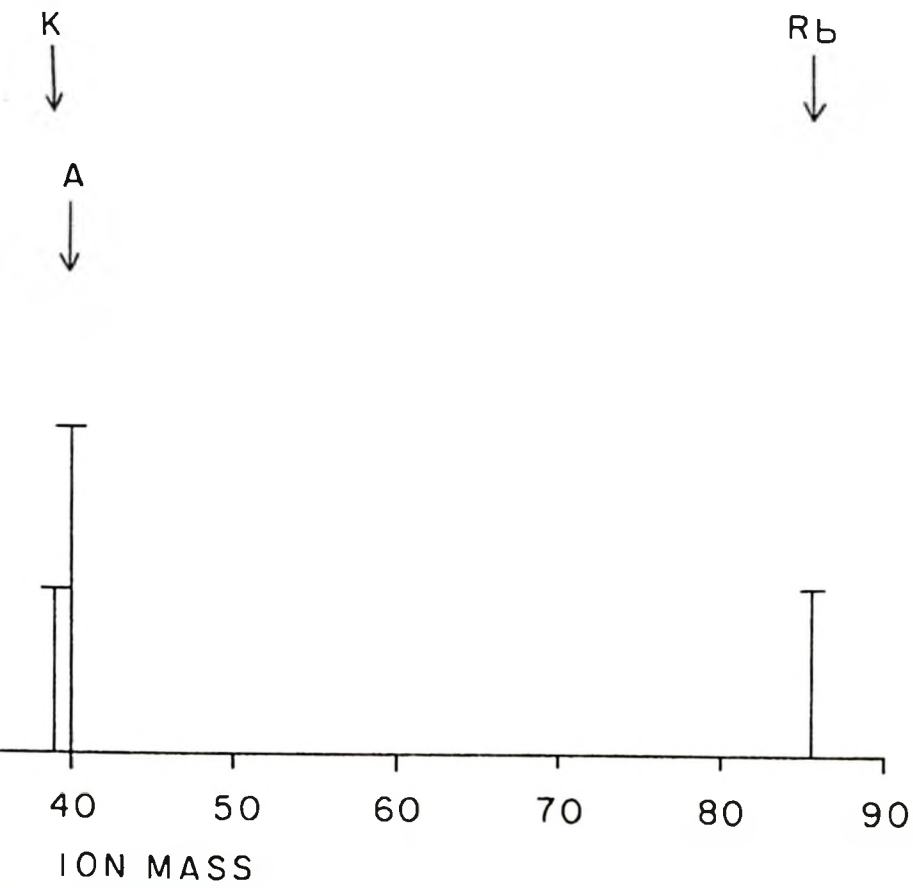
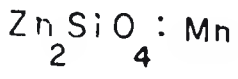
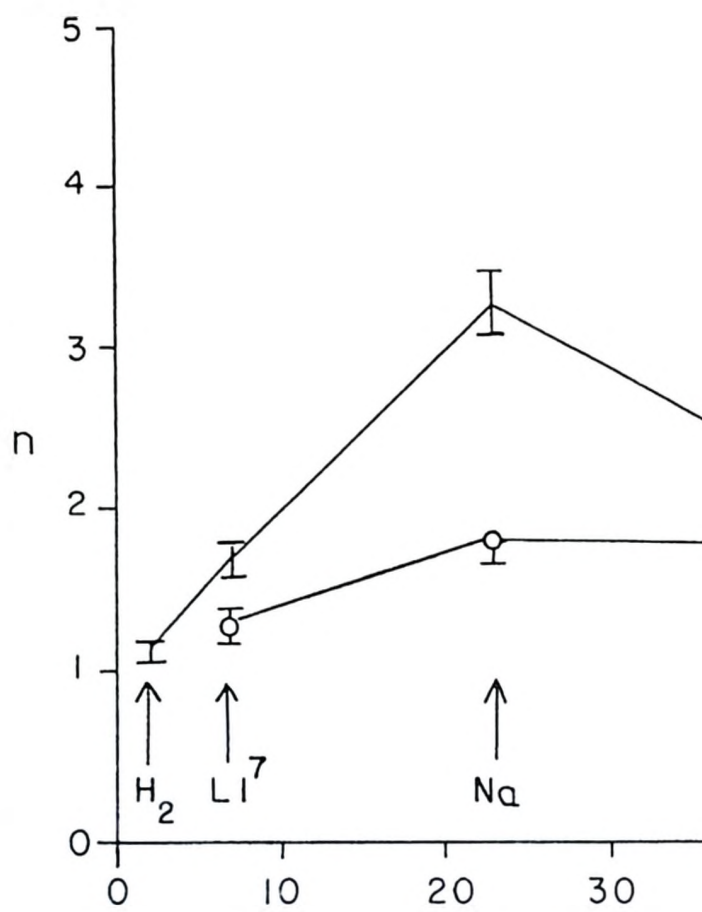


Fig. 22

n versus ion mass. The upper curve is for ZnS:Ag,
the lower curve for $\text{Zn}_2\text{SiO}_4\text{:Mn}$.



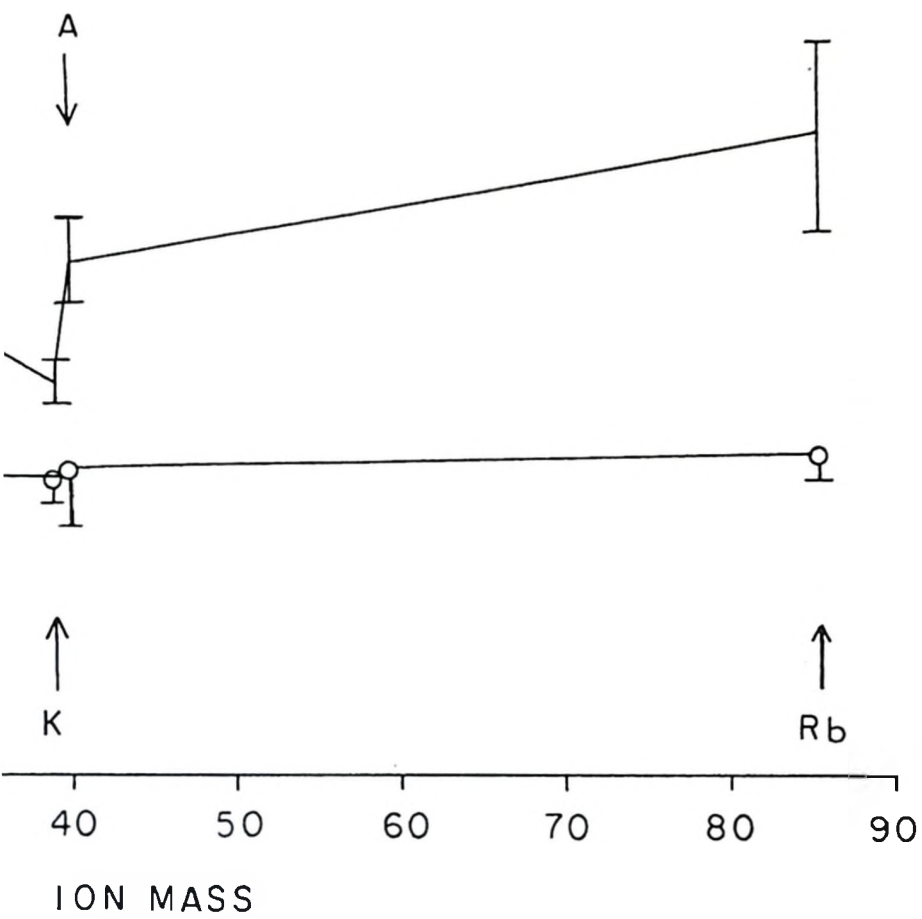


Fig. 23

L versus ion mass for ZnS:Ag. The top curve is for 20 KeV ions, the middle curve for 15 KeV ions and the bottom curve for 10 KeV ions. The points plotted at zero mass are for electrons.

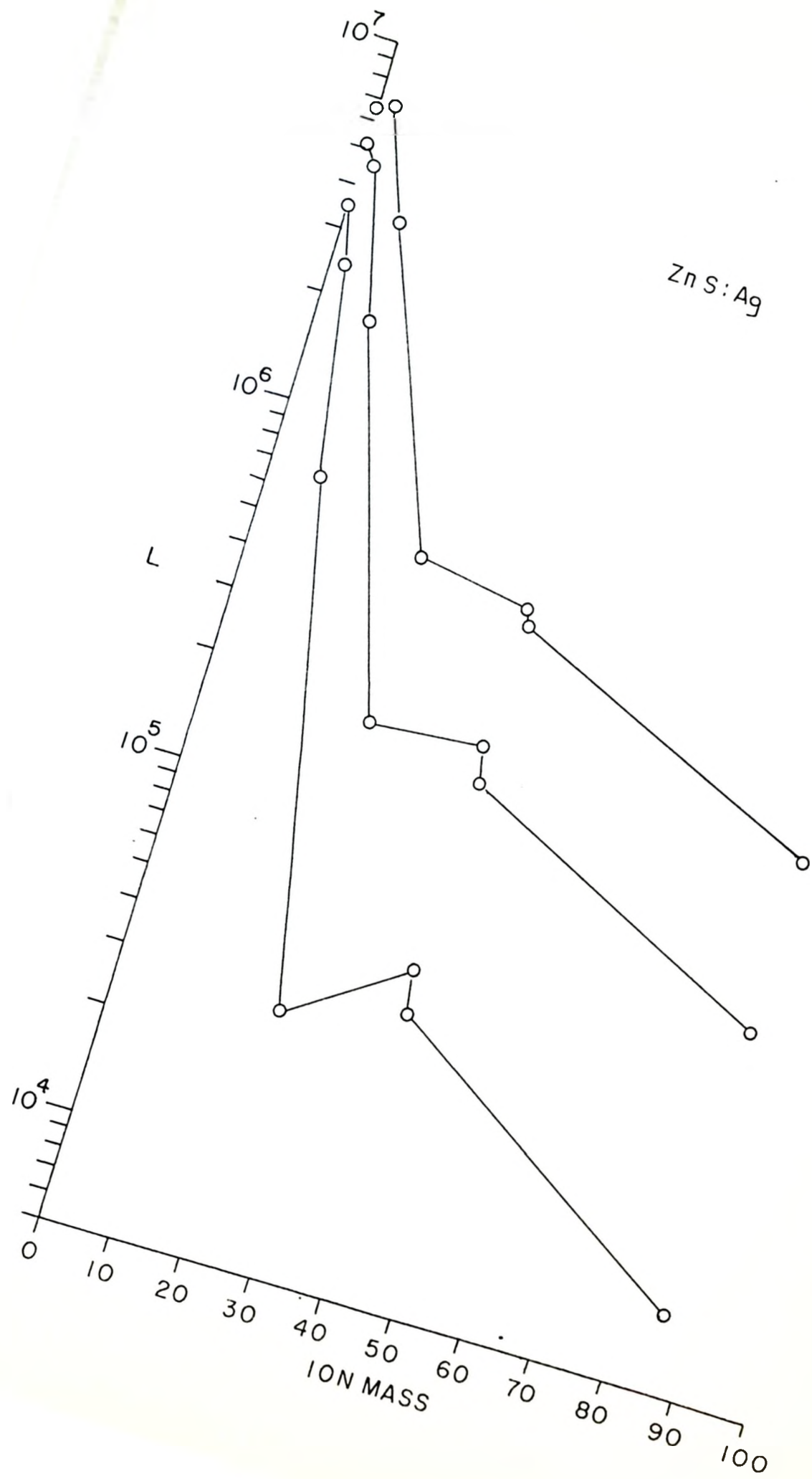


Fig. 24

L versus ion mass for $\text{Zn}_2\text{SiO}_4:\text{Mn}$. The top curve is for 20 KeV ions, the middle curve for 15 KeV ions and the bottom curve for 10 KeV ions. The points at zero mass are for electrons.

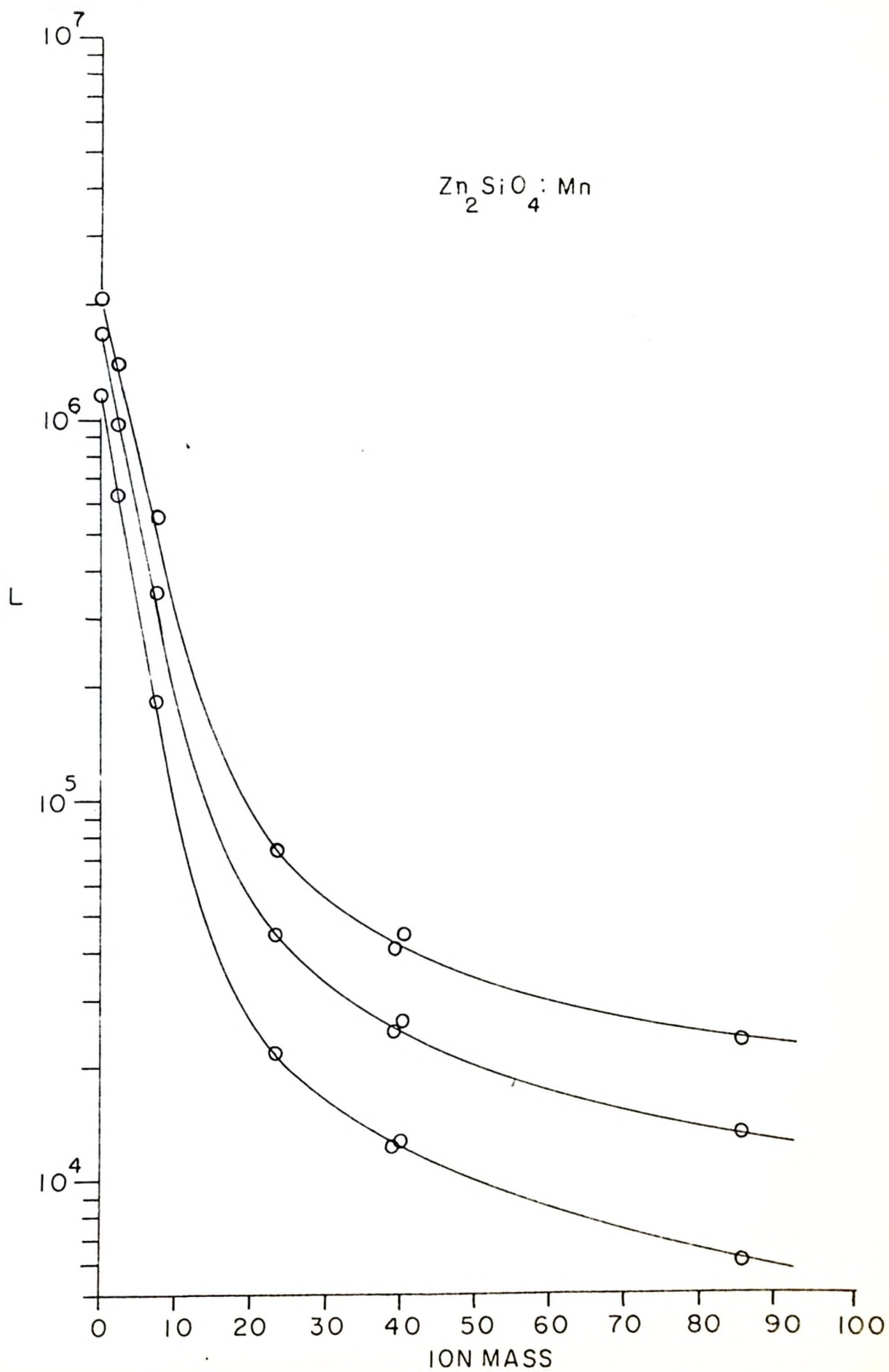
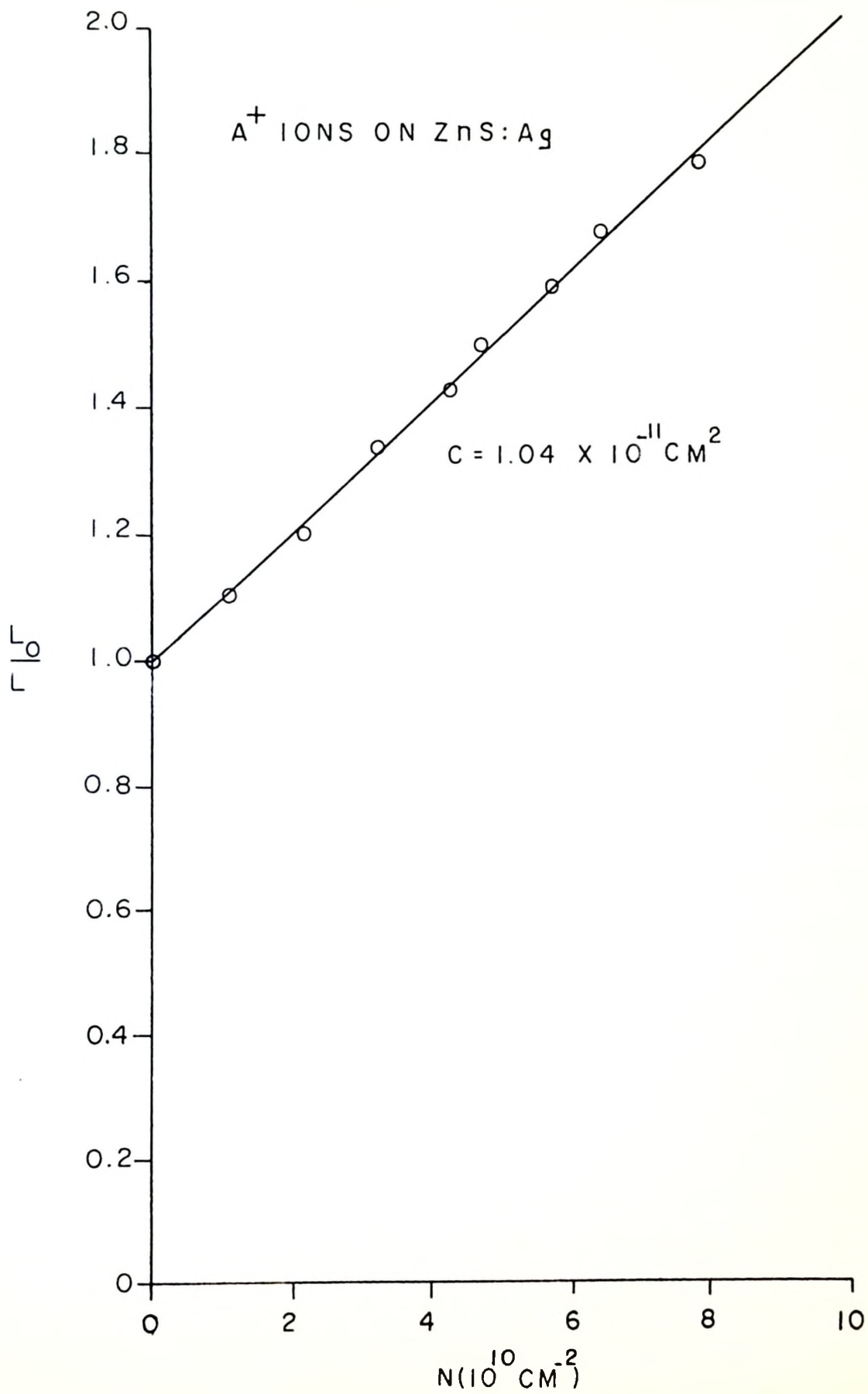


Fig. 25

The deterioration of ZnS:Ag under A^+ ion bombardment.
 L_0/\bar{L} is the ratio of the initial light output to
that after bombardment with N ions per cm^2 .



Chapter IV

Discussion of the Results of Chapter III

1. Efficiency

To the best of the writer's knowledge, the only other work in which the luminescence of phosphors under positive ion bombardment has been determined as a function of the ion energy, for energies comparable with those used here, is that of Hanle and Rau (1952). Hanle and Rau found that for ZnS:Ag under bombardment with H_2^+ ions the light output was approximately proportional to the ion energy for energies in the range 15 - 35 KeV. This is in approximate agreement with the results for H_2^+ ions found here. Hanle and Rau also made an absolute determination of the luminescence efficiency of ZnS:Ag and $Zn_2SiO_4:Mn$ under bombardment with various ions. Each of these determinations was made at an ion energy between 20 and 30 KeV. The results of the previous chapter show that, except for H_2^+ ions, the efficiency is a sensitive function of the ion energy. The energy dependence of the efficiency was not taken into account by Hanle and Rau.

Using the values found by Hanle and Rau for the efficiency of ZnS:Ag under H_2^+ ion bombardment and the efficiency of $Zn_2SiO_4:Mn$ under A^+ ion bombardment, the

efficiency of these phosphors at 25 KeV under bombardment with the other ions can be calculated from the relative L values. The results are shown in table III.

Table III

Ion	Efficiency at 25 KeV (%)	
	ZnS:Ag	Zn ₂ SiO ₄ :Mn
H ₂ ⁺	25	
Li ⁷⁺	15	9.2
Na ⁺	3.3	1.3
K ⁺	2.3	0.8
A ⁺	2.2	0.8
Rb ⁺	1.0	0.4

Apart from the two values used to normalize the present results to an absolute scale, the only value in table III which was also determined by Hanle and Kau is the efficiency of ZnS:Ag under A⁺ ion bombardment. Their value is 3.4%. The apparent discrepancy is greatly reduced if the efficiency is calculated for 30 KeV (the upper limit of the energy range in which the determinations of Hanle and Kau were made). Extrapolation of the results for A⁺ ions given in Chapter III gives a value of 3.2% for the efficiency at 30 KeV, compared with 2.2% at 25 KeV.

If the relationships are extrapolated to sufficiently high energies, efficiencies of 100% are predicted. Obviously the validity of the relationships must break down before

such a value of E is reached. These values of E are given for the different ions in table IV.

Table IV

Ion	E (KeV) ZnS:Ag	E (KeV) Zn ₂ SiO ₄ :Mn
H ₂ ⁺	78.5	
Li ⁷⁺	70.5	141
Na ⁺	64.8	279
K ⁺	109	416
A ⁺	78.0	360
Rb ⁺	75.0	443

2. Interpretation of E_0

Within the range of energies studied, the variation of light output with ion energy is shown by the results of Chapter III to be of the form

$$L \propto (E - E_0)^n, \quad (19)$$

where the constants E_0 and n depend on the nature of the phosphor and the bombarding ions. If this relationship can be extrapolated down to zero light output, then E_0 is to be interpreted as a threshold energy. The relationship (19) is of the same form as that governing the variation of cathodoluminescence with electron energy. (See, for example,

the review article by Garlick, 1950). In the case of cathodoluminescence the threshold energy has been ascribed to surface contamination of the phosphor. A similar interpretation of E_0 in the case of ion bombardment does not seem plausible, however. If E_0 were the energy required by an ion to penetrate a dead surface layer of the phosphor sample, one would expect E_0 to increase rather rapidly with increasing ion mass. This expectation is not fulfilled. The results shown in fig. 20 indicate that for ZnS:Ag there is no significant trend of E_0 with ion mass. A line at 3.5 KeV just passes within the experimental limits of all the points in fig. 20 except that for argon. The range of ion mass for these points is from 2 for H_2 to about 85 for Rb. In fig. 21, for $Zn_2SiO_4:Mn$, it can be seen that E_0 is greatest for the lightest ion shown, namely Li^{7+} .

The experiment described in section 4 of Chapter III also has a bearing on the physical interpretation of E_0 . In this experiment a region of the phosphor sample was subjected to prolonged bombardment with K^+ ions of energy 6 KeV. This energy is only about 2 KeV above the threshold value E_0 . Hence, as one would expect, only a very small light output was obtained. The 85% by which this light output fell during the course of the bombardment is taken as a measure of the deterioration of the phosphor in the region penetrated by the 6 KeV ions. It was observed that the response of the

phosphor to 12 KeV ions was reduced by about 83% as a result of the 6 KeV bombardment. If the deterioration of the phosphor is confined to a well defined region corresponding to the depth of penetration of the 6 KeV ions -- as the results of Young (1955) suggest -- then it follows that practically all the light output normally due to a 12 KeV ion originates in this region. Hence it is during the latter portion of its range that a 12 KeV ion does not give rise to luminescence. This suggests that the constant E_0 is not associated with any dead surface layer, but is a true threshold energy such that an ion having energy less than E_0 cannot excite luminescence in any part of the phosphor.

3. Theory

In order to compare the observed relation between light output and ion energy with the predictions of theory, a theoretical expression must be found for the rate of electronic excitation in a solid due to the passage of an incident heavy particle. The well known formula of Bethe¹ for $-dE_x/dx$ is inapplicable here because it does not take into account the phenomenon of charge exchange which causes the average charge of the incoming particle to approach zero for small velocities. If the values of velocity

¹See, for example, Fermi (1950)

appropriate to these experiments are substituted into the Bethe formula the value given for $-dE_x/dx$ is in most cases negative.

The incident particle velocities used in these experiments are all less than v_0 , the orbital velocity of the electron in a ground state hydrogen atom, viz. 2.19×10^8 cm/sec. In table V are listed the values of the velocity v of various ions at an energy of 25 KeV.

Table V

Particle	Mass (amu)	v (cm/sec) at $E = 25$ KeV
H ₂	2	1.55×10^8
Li ⁷	7	8.29×10^7
Na	23	4.58×10^7
K	39	3.52×10^7
A	40	3.47×10^7
Rb	85.5	2.37×10^7

According to Nielsen (1956), when $v < \frac{1}{2}v_0$ the cross section for electron capture is so large that the incoming particles can be regarded as uncharged throughout the penetration of the solid. Table V shows that this condition is well satisfied here except for H₂ at the upper end of the energy range. When the incoming particle is neutral, most of its energy is expended by elastic collisions with the lattice atoms, and only a fairly small fraction is dissipated by electronic excitation. It is just this small fraction, however, which will contribute to the luminescence in ZnS:Ag, for this luminescence arises from the capture of conduction

electrons (or free holes) by the luminescence centres.

In most of the published theoretical work dealing with the slowing down of low velocity atomic particles in solids, the energy loss due to electron excitation has been considered only to the extent necessary to show that it is negligible compared with the energy loss due to elastic collisions. The subject has therefore received only rather qualitative treatment. To the best of the writer's knowledge, the work in which this aspect has been considered in most detail is that of Seitz and Koehler (1956). In this work an expression is derived for the probability, P , that an electronic transition will be induced in a stationary atom by the close passage of a slow atomic particle. The expression is

$$P = \frac{P_0}{v^2} \exp(-W^2 R^2 / 2\hbar^2 v^2). \quad (20)$$

The constant P_0 involves only terms that are constant for a given incident particle and a given stationary atom. v is the velocity of the moving particle and W is the energy of the electronic transition being considered. In the derivation it is assumed that P is constant if the impact parameter p is less than some constant R , and zero if p is greater than R . R may therefore be defined as the range of the interaction. The assumption of a sharply defined interaction range is most nearly justified in the case when the

moving particle is uncharged so that there is no long range Coulomb interaction. As was pointed out above, this is just the case we are concerned with here.

Equation (20) can be written in the form

$$P = \frac{P_0}{E_x} \exp\left(-\frac{w^2 R^2}{8R_H a_0^2 E_x} \cdot \frac{M}{m}\right), \quad (21)$$

where E_x is the energy of the moving particle, R_H is the Rydberg energy, a_0 is the radius of the first Bohr orbit in hydrogen, m is the electronic mass and M is the mass of the moving particle.

As the density of lattice atoms is constant, the total number of electronic excitations produced in the phosphor by a single incident particle is proportional to

$$\int_0^X P dx, \quad (22)$$

where X is the range of the incident particle. Because P is given as a function of the energy E_x , the relationship between E_x and x must be known before the above integral can be evaluated. This relationship will be governed not by electronic excitation but by the elastic collisions, which constitute the dominant mechanism of energy loss. Nielsen (1956) shows that under these conditions $-dE_x/dx$ is a constant independent of energy. He gives references to experimental work confirming this result. Additional

confirmation is given by Young (1955). The integral (22) can therefore be written

$$K \int_0^E P dE_x,$$

where E is the incident energy and K is a constant. By substitution for P from equation (21), this expression becomes

$$KP_0' \int_0^E \frac{1}{E_x} \exp(-C/E_x) dE_x, \quad (23)$$

where

$$C = \frac{W^2 R^2}{8R_1 a_0^2} \cdot \frac{M}{m}. \quad (24)$$

By making the substitutions

$$C/E_x = t \quad \text{and} \quad C/E = z, \quad (25)$$

the integral in expression (23) may be written

$$\int_z^\infty \frac{e^{-t}}{t} dt. \quad (26)$$

This integral is the well known exponential-integral, $-Ei(-z)$, for which tabulated values are available.

If it is assumed that the luminescence per incident ion, L , is proportional to the number of conduction electrons produced per incident ion, then it follows that

for a given type of ion

$$L \propto -\text{Ei}(-z) = -\text{Ei}(-C/E). \quad (27)$$

4. Comparison of Theory with Experiment

Relative values of L as given by (27) can be plotted against the incident energy E once a value of C is chosen. It was found that by choosing appropriate values for C the theoretical curves could be made to fit the experimental curves for ZnS:Ag to a surprising degree of accuracy. Two examples are shown in figs. 26 and 27, for Li^{7+} and H_2^+ ions respectively.

The form of the function $-\text{Ei}(-C/E)$ is such that the value of L increases more rapidly with E for larger than for smaller values of C . From equation (24) it can be seen that if R is a not very sensitive function of the ion mass then C increases with increasing ion mass. This then accounts for the observation that the exponent n in the empirical relation between L and E increases with increasing ion mass, the case of Na being excepted. Actually, in order to obtain the best fit to the experimental curves, C had to be chosen in such a way as to imply a small variation of R with ion mass. For the chosen value of C the corresponding value of R was calculated from equation (24) using $W = 3$ eV for the energy of the band to band transition in ZnS. The values of R so obtained are shown in table VI.

Table VI

Incident particle	Mass (amu)	R (Å)
H ₂	2	3.23
Li ⁷	7	2.43
Na	23	1.95
K	39	1.25
A	40	1.20
Rb	85.5	1.02

For the last three particles listed in table VI, the values of R are somewhat less than the radii of the corresponding atoms. Probably all the values of R are too low. However, the order of magnitude for R seems reasonable. It is conceivable that the steady decline of R with increasing mass of the incident particles might be due to decreasing average charge of the particle. For a given energy the assumption of zero charge during penetration of the phosphor is better justified for incident particles of higher mass (see table V). The effective interaction range will increase with increasing average charge because of the long range nature of the Coulomb interaction.

Because of the good fit of the theoretical curves to the experimental points, the theory indicates the

existence of the threshold energies to the same extent that they are implied by the experimental results. Thus if the theoretical expression in the case of Li^{7+} ions is plotted against $E - 4 \text{ KeV}$, the curve obtained on a logarithmic scale is linear to a high degree of accuracy over most of the range of E used in the experiment, but shows a tendency to level off at the upper end of this range. In fig. 27 for H_2^+ ions, the theoretical curve is plotted on a linear scale down to zero energy. The prediction of an effective threshold energy is clearly illustrated here, for the curve remains very close to the axis for small values of E , and then turns up sharply in a small energy interval, after which it remains approximately linear over a large range of E . For values of E close to the upper end of the energy range the condition $v < \frac{1}{2}v_0$ is not well fulfilled (see table V). This may account for the discrepancy between theory and experiment in this region.

In the foregoing theory it was assumed that the probability that a free electron (or hole) would give rise to a luminescence quantum was independent of the location of the electron (or hole) in the phosphor crystal. In fact this may not be true. The results of Young (1955) indicate that the range of 20 KeV A^+ ions in ZnS:Ag is about 0.05 microns. This is only about 90 times the lattice spacing in ZnS . Thus the free electrons and holes are produced

very close to the crystal surface. It is possible that the density of centres at which non-radiative recombination of electrons and holes can occur may increase as the surface of the crystal is approached (see Garlick, 1950). This effect would contribute to the large value of n found for heavy ions. The possible existence of such an effect could be investigated by means of experiments in which the dependence of n on the angle of incidence of ions bombarding a single crystal phosphor sample was studied. However, the foregoing work seems to suggest that such a surface effect is not essential to the explanation of the high values of n found for heavy ions.

Fig. 26

Comparison of theory with experiment. The solid line represents relation (27) with $C = 22.2 \text{ KeV}$ and a suitably chosen proportionality constant. The experimental points are for Li^{7+} ions on ZnS:Ag .

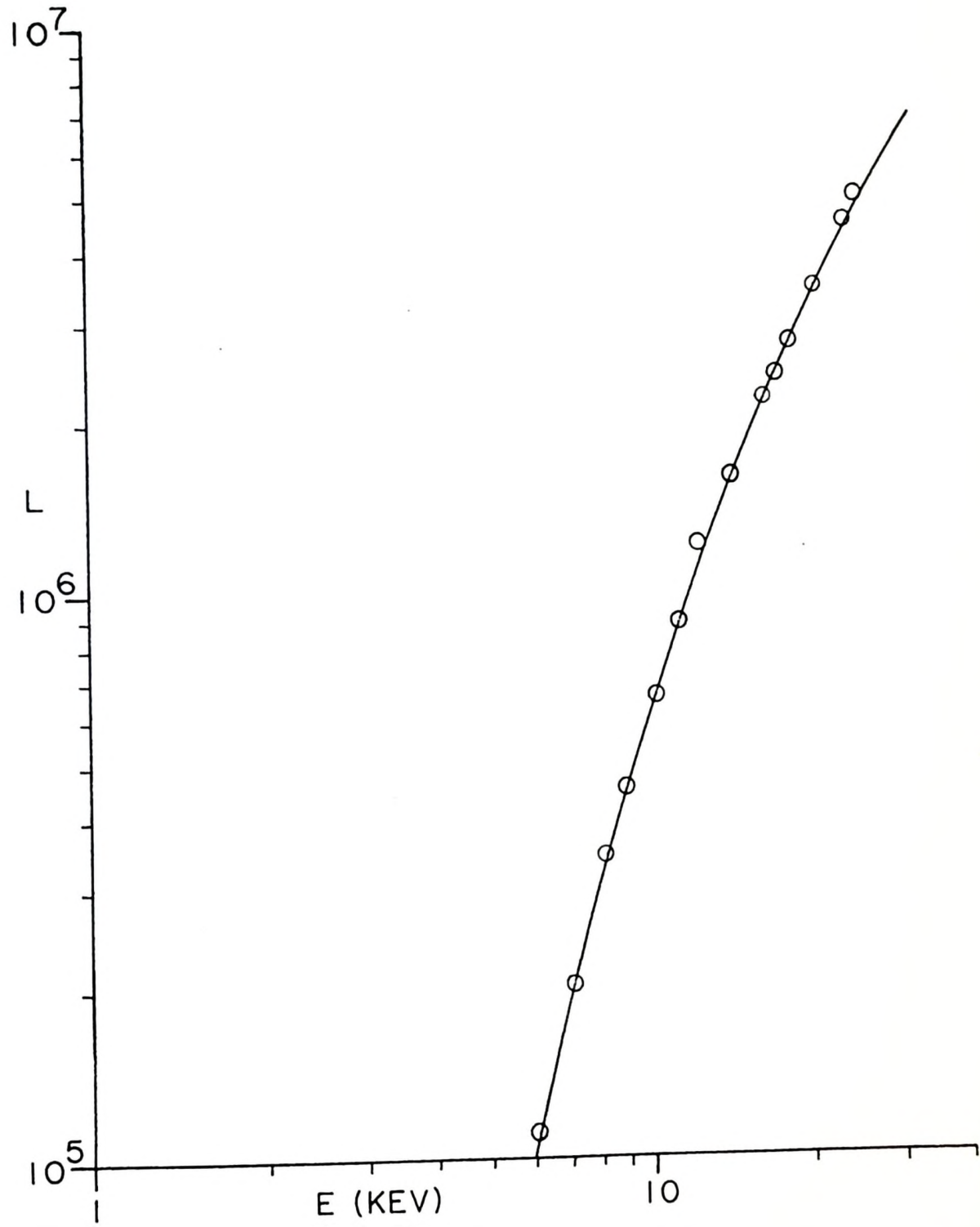
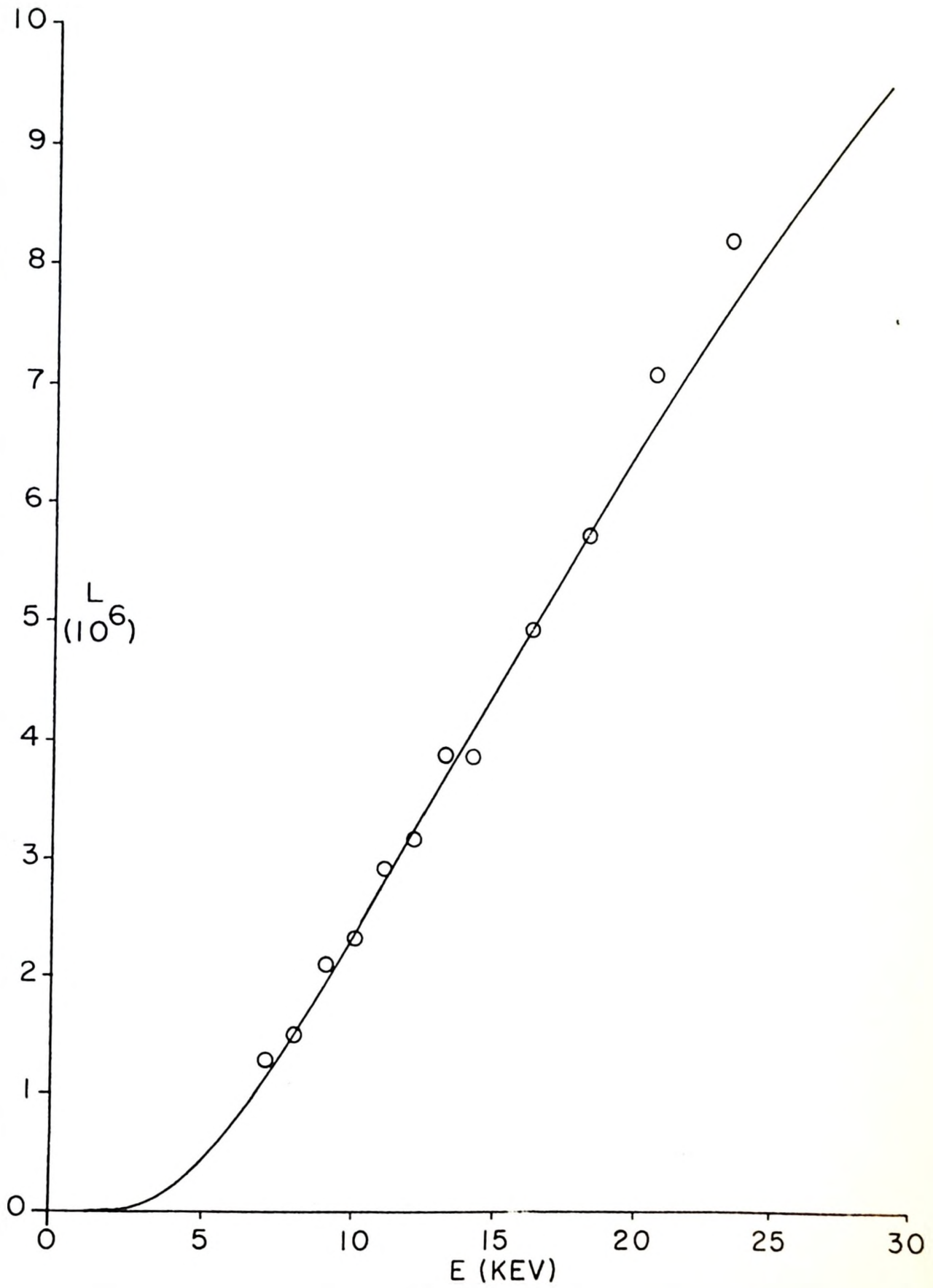


Fig. 27

Comparison of theory with experiment. The solid line represents relation (27) with $C = 11.2$ KeV and a suitably chosen proportionality constant. The experimental points are for H_2^+ ions on ZnS:Ag.



Summary

The light emitted from one side of samples of ZnS:Ag when the other side is bombarded with K^+ ions was studied as a function of the sample thickness. A theory that is in fairly good agreement with the experimental results is presented.

The luminescence response of samples of ZnS:Ag and $Zn_2SiO_4:Mn$ to bombardment with various ions was determined as a function of the ion energy. Within the range of ion energies studied ($E < 25$ KeV) the luminescence response, L , is related to the ion energy, E , according to

$$L \propto (E - E_0)^n.$$

E_0 is a threshold energy which, in the case of ZnS:Ag, is not a very sensitive function of the ion mass. The values of E_0 for H_2^+ , Li^{7+} , Na^+ , K^+ , A^+ and Rb^+ ion bombardment of ZnS:Ag are all a few KeV. In the case of $Zn_2SiO_4:Mn$, E_0 is approximately zero for Na^+ , K^+ , A^+ and Rb^+ ions, but is about 2.5 KeV for Li^{7+} ions. The exponent n depends on the nature of the phosphor and of the bombarding ions. The value of n tends to increase with increasing ion mass. The experimental results for ZnS:Ag are consistent with a theory in which it is assumed that the bombarding particles penetrate

the phosphor as neutral atoms and lose a small fraction of their energy by electronic excitation of the atoms of the phosphor due to small impact parameter collisions.

References

- BERTHOLD, W. 1955. *Naturwissenschaften*, 42: 436.
- BROSER, I. and WARMINSKY, R. 1951. *Z. Naturforschung*, 6A: 85.
- DEWDNEY, J.W. 1955. Ph.D. Thesis, McMaster University.
- FERMI, E. 1950. *Nuclear Physics*. University of Chicago Press.
- GARLICK, G.F.J. 1950. *Advances in Electronics*, II. Academic Press Inc., New York.
- HANLE, W. and RAU, K.H. 1952. *Z. Physik*, 133: 297.
- KLASENS, H.A. 1946. *Nature*, 158: 306.
- LAMBE, J. 1955. *Phys. Rev.* 98: 985.
- LAMBE, J. and KLICK, C.C. 1955. *Phys. Rev.* 98: 909.
- MARTIN, W. 1957. *Z. Physik*, 147: 582.
- NIELSEN, K.O. 1956. *Electromagnetically Enriched Isotopes and Mass Spectrometry*, edited by M.L. Smith. Butterworths Scientific Publications, London.
- RICHARDS, P.I. and HAYS, E.E. 1950. *Rev. Sci. Instr.* 21: 99.
- SEITZ, F. 1939. *Trans. Faraday Soc.* 35: 74.
- SEITZ, F. 1949. *Disc. Faraday Soc.* 5: 271.
- SEITZ, F. and KOEHLER, J.S. 1956. *Solid State Physics*, 2, edited by F. Seitz and D. Turnbull. Academic Press Inc., New York.
- SMITH, A.W. and TURKEVICH, J. 1954. *Phys. Rev.* 94: 857.
- YOUNG, J.R. 1955. *J. Appl. Phys.* 26: 1302.